

2-6 Further Considerations

Further considerations regarding Ghuzayn, Sarami and Hara Kilab area are presented in Chapter 3 (Section 3-6).

2-6-1 Mahab area

Fig.II-2-49 shows the compiled geophysical map obtained in Mahab area.

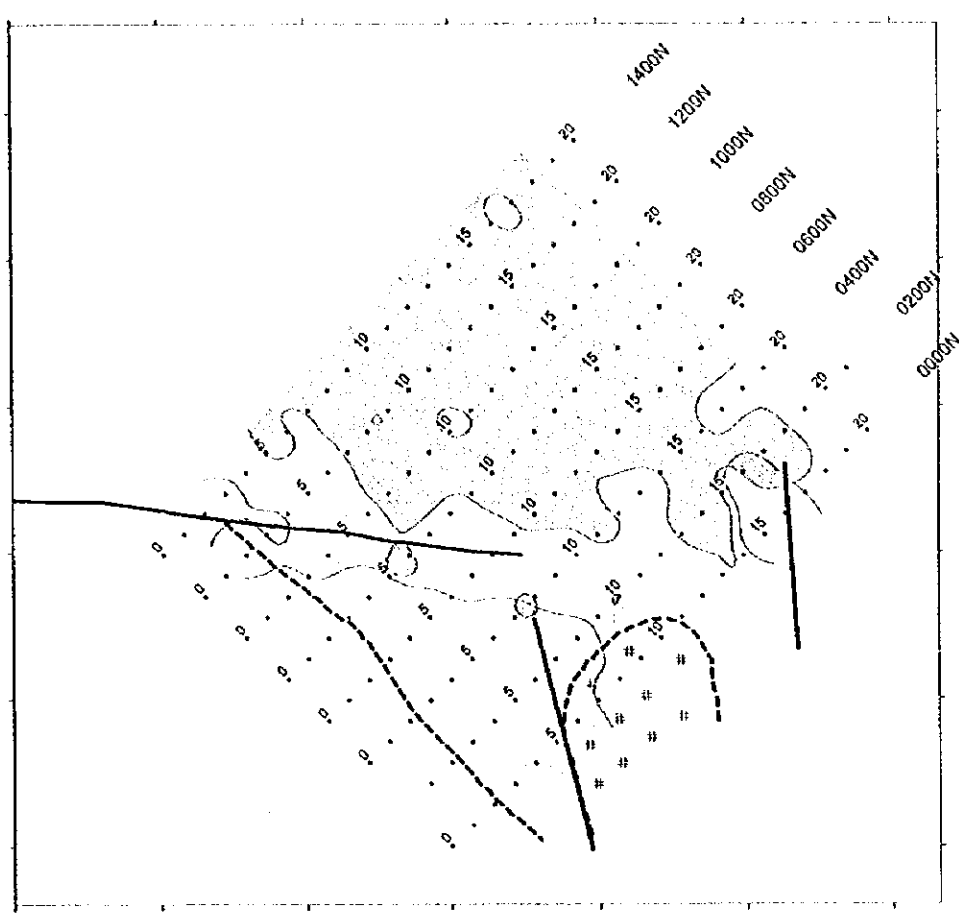
The IP results indicate a high chargeability zone of more than 8 mV/V detected in the southern part of the area. The distribution of this zone closely corresponds to that of V1-1. The high metal factor anomaly widely distributed in the north half of the area is probably due to a geological occurrence not related to mineralization, judging from the fact that the calculation of the metal factor anomaly is not based on the occurrence of chargeability anomalies.

2-6-2 Maqail area

Fig.II-2-50 shows the compiled geophysical map obtained in Maqail area.

The IP results indicate high chargeability zones, of more than 8 mV/V, being extended along N-S direction in the central and western parts of the area. The central anomaly is seen nearly distributed along the faults observed in the upper extrusive rocks (V1-2) in an N-S direction. The western anomaly is detected in the trondhjemite and/or on the boundary V1-1 and V1-2. The high metal factor zone is recognized only at a narrow portion on the boundary between V1-1 and V1-2 in the western part of the area. There is no possibility of the existence of massive sulphide deposits, since any evident low resistivity zone was not delineated in the area. However, further geophysical survey is recommended in order to investigate the north extension of the high chargeability zone detected in the central part of the area.

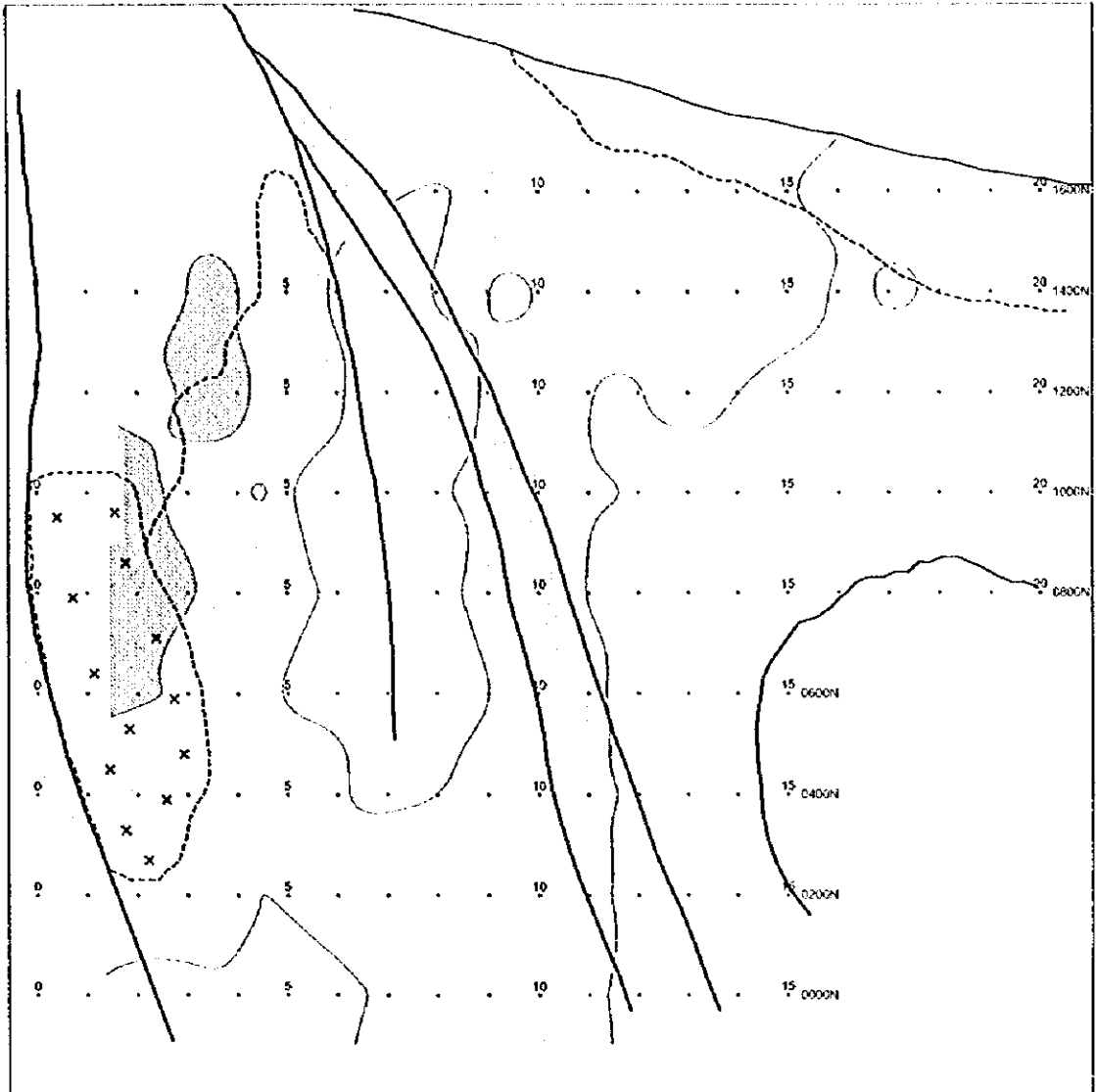




- : Chargeability Anomaly(8mV/V<)
- : Metal Factor Anomaly(25<)
- - - : Geological Boundary
- / : Fault
- ⊗ : Gabbro

Fig. II -2-49 Compiled geophysical map in Mahab area










-  : Chargeability Anomaly(8mV/V<)
-  : Metal Factor Anomaly(25<)
-  : Geological Boundary
-  : Fault
-  : Toronjomite

Fig. II -2-50 Compiled geophysical map in Maqail area



CHAPTER 3 TEM SURVEY

3-1 Background and Objectives

The TEM (Transient Electro-Magnetic) survey, sensitive to conductive bodies, such as massive sulphide deposits, was conducted to clarify the nature of the sulphide mineralization within the area delineated by the results of the TDIP survey.

During the present survey, large fixed loops were located on the base of the anomalies extracted from the TDIP survey. Taking into consideration the remarkable response given by conductive materials, such as massive sulphide ores, this detailed method is useful to extract promising mineralization zones by estimating their locations and boundaries.

3-2 Survey Locations and Specifications

The geophysical TEM survey method was utilized in Ghuzayn, Hara Kilab and Sarami areas by using large fixed loops. In relation to the amount work undertaken during the TEM survey, a total of 14 loops corresponding to 1,134 stations were carried out in this year, as indicated in Table II-3-1.

3-3 TEM Survey Method

3-3-1 Basic principles

The principle of the TEM system used in this survey is to energize an ungrounded loop situated on the surface of the earth, as illustrated in Fig.II-3-1. When the currents flowing in the loop are switched off, free electron conduction currents are induced (eddy currents) in the ground. The eddy currents are known to depend on the conductivity, size and shape of the conductive body, and position with respect to the sensing loop. These eddy currents set up a secondary magnetic field which can be detected by a receiver coil as a time-dependant decaying voltage (Fig.II-3-2). The measurement of the time dependent decaying voltage is a means of detecting conductors in the ground. This transient decay can be measured by a number of measurement channels recording the voltage at various delay times after the transmitted fields are switched off. According to Faraday's law, the quick shut-off of the primary magnetic field caused by the current termination induces a pulse of e.m.f. (voltage) in the surrounding media. The resulting eddy currents produced in nearby conductive material support a surrounding secondary magnetic field for the duration of the pulse. Thereafter, with no external e.m.f. to support it, this system of currents and magnetic field decays with time, and it is this transient magnetic field which the receiver measures. These measurements occur during fixed time "windows" which occupy most of the "off-time" of the transmitter. As the receiver must know when the transmitter is off, synchronization was done by using crystal clocks.

Table II-3-1 Survey amounts of TEM

| AREA | Number of Loops | Number of Points |
|--------------|-----------------|------------------|
| Ghuzayn | 1 | 81 |
| Hara Kilab | 5 | 405 |
| Sarami | 8 | 648 |
| Total | 14 | 1134 |

Table II-3-2 Channel times after switch off

| Channel No. | Sampling time | Window width |
|-------------|---------------|--------------|
| 1 | 88 μ s | 18 μ s |
| 2 | 107 | 24 |
| 3 | 131 | 36 |
| 4 | 162 | 37 |
| 5 | 201 | 40 |
| 6 | 251 | 72 |
| 7 | 314 | 76 |
| 8 | 396 | 100 |
| 9 | 499 | 142 |
| 10 | 631 | 156 |
| 11 | 799 | 180 |
| 12 | 1014 | 250 |
| 13 | 1287 | 380 |
| 14 | 1636 | 390 |
| 15 | 2081 | 500 |
| 16 | 2648 | 720 |
| 17 | 3373 | 780 |
| 18 | 4297 | 1080 |
| 19 | 5475 | 1420 |
| 20 | 6978 | 1560 |

Table II-3-3 Specifications of TEM survey instruments

| Items | Specifications |
|-----------------|--|
| Transmitter | Max output,30A,180V |
| Generator | 5HP,120V,3phase,400Hz |
| Receiver | 25Hz:0.088-7.19ms 6.25Hz:0.35-28.7ms 2.5Hz:0.88-71.9ms |
| Magnetic Sensor | Induction coil Effective area 100m ² |
| Recorder | Protem,2Mb |

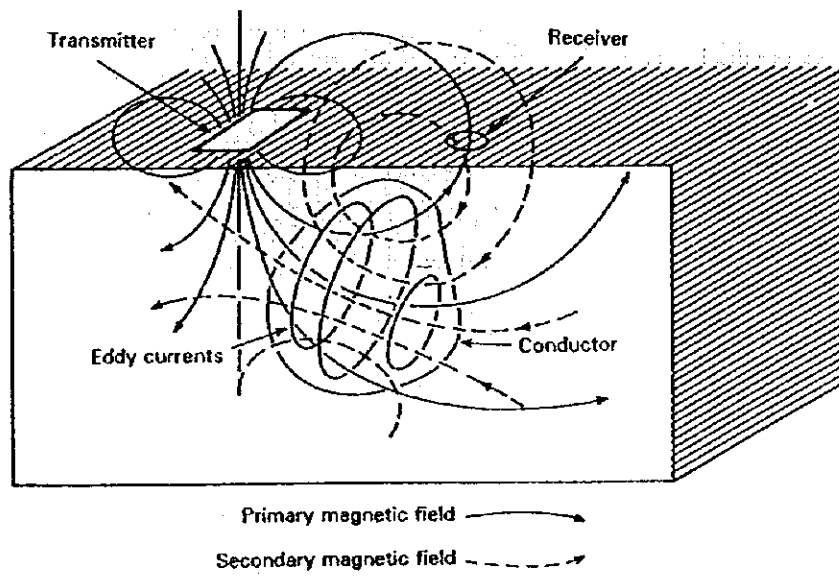
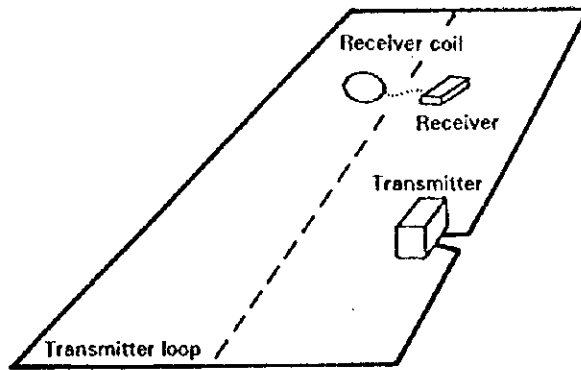


Fig. II-3-1 Schematic TEM survey configuration

3-3-2 Logistics and data acquisition

There are several varieties of TEM systems and modes of operations. During this survey it was used the configuration of large fixed-loop. For the case of large loops, a large, single-turn square loop of wire of 600m by 600m is laid out on the ground. A portable power generator of 2500W fed a transmitter, which provides a series of alternating bipolar currents pulses with slow exponential turn-on and a rapid linear turn-off precise current waveform through the loop. After the transmitter loop has been set up, a small portable multi-coil receiver is moved to stations along surface lines inside the loop. Lines were surveyed within the loop to a distance of 100m away from the loop and the grid interval between the observed points was 50m.

Previous to the data acquisition, the crystals of the transmitter and receiver are warmed up before attempting to synchronize. Synchronization of the transmitter and receiver was carried out using the built-in high stability quartz crystal oscillators. Integration for each measurement was carried out over 2^8 cycles.

The current waveform driven through the transmitter loop and the number of spacing of channels in the receiver are the main distinguishing features of this method. 20 time channels with locations and width are shown in Table II-3-2. Successive operations at 25Hz, then 2.5Hz, effectively gives 30 channels covering range from 88μ sec. to 72 msec. A steady current is terminated rapidly by a 220μ sec. ramp in large loops.

During data collection, several transient decays are recorded for each sounding. Readings are acquired at several receiver gains with opposite receiver polarities for each sounding location to eliminate any cultural noise. Many pulses of positive and negative polarities are stacked in a short period of time and averaged to remove any disturbance.

3-3-3 Equipment specifications

The EM37 system manufactured by Geonics Ltd. of Canada was utilized during the TEM survey of this year with the specifications as detailed in Table II-3-3. The receiver used is the Protem.

The current waveform in the transmitter consists of alternating bipolar current pulses with a slow exponential turn-on and a rapid linear turn-off. The base frequency of operation can be set at 2.5, 6.25 or 25 Hz, with corresponding window times of 71.9, 28.7, or 7.17 msec respectively. In this survey we used a base frequency of 25 Hz transmitter motor generator: 5 HP Honda gasoline engine coupled to 120 volt, 3 phase, 400Hz alternator.

At the receiver the induced voltage in the coil is measured in millivolts. Using the effective area of the coil and the gain of the receiver, these measurements are converted to the time derivative of the magnetic field in nanovolts/amp-meter².

3-4 Analysis Method

The fact that the primary field is absent during measurement time, leads to "cleaner" data which is easier to interpret. The rate of decay of a conductor's magnetic field depends primarily on its size

and conductance. Eddy currents decay rapidly in poor conductors, while those due to good conductors decay slowly, and the timing of the channels is such that only the effects of eddy currents due to the good conductors are seen in the later channels. In conductive environments, therefore, the response from overburden and weak mineralization should be minimal in the later channels where the target response predominates.

The first step in data processing is to average the e.m.f. (voltages) that are recorded at opposite receiver polarities. Then, the records at different amplifier gains are combined to give a single composite transient decay. After the composite transient decay has been calculated for each measurement point, the late stage apparent resistivities are calculated by using the following equation:

$$\rho_a(t) = \frac{\mu^{5/3} M_r^{2/3}}{20^{2/3} \pi} \cdot \frac{M_t^{2/3}}{t^{5/3} V^{2/3}}$$

Where V is the voltage measured at the receiver, M_r is the moment of the receiver, M_t is the moment of the transmitter, μ is magnetic permeability, and t is the time measured after transmitter switch off.

The TEM response detected in the receiver, depends not only on the electrical properties of the ground, but also on the location of receiving points and transmitter loop size, generally the highest response are observed at the center of the loop. To correct the response due to the receiving location, the following procedure was carried out:

From the TEM data obtained at the center of the transmitter loop, a layered resistivity structure was calculated by using an inversion analysis that assumes that this electrical structure represents an average resistivity in the loop.

By using the parameters of this resistivity structure, a synthetic response $B_c(x, y)$ was calculated at all the points within the loop by taking also into account the relative position between the receiver and transmitter loop. If the resistivity structure at a point is nearly same as the average resistivity structure, the observed EM response should be almost the same as the calculated synthetic response, resulting in a minimal difference. On the contrary and if the average resistivity structure is not related to an anomaly but the point represents the location of the conductive body underlied, then the response becomes extremely high as compared with the synthetic response, and therefore, the difference between the responses becomes high, i.e.,

$$B(x,y) = \log (B_o(x,y) / B_c(x,y))$$

Where: $B(x,y)$ is the difference of response, $B_o(x,y)$ is the observed response, $B_c(x,y)$ is the synthetic response, and \log is the logarithm of base 10 (Fig.II-3-3).

Contour map of the difference in the TEM responses permit the clarification of anomalies (if any) by the contrast in the TEM response values.

For the depth estimation, the following formula is used:

$$d = \sqrt{500 \rho t}$$

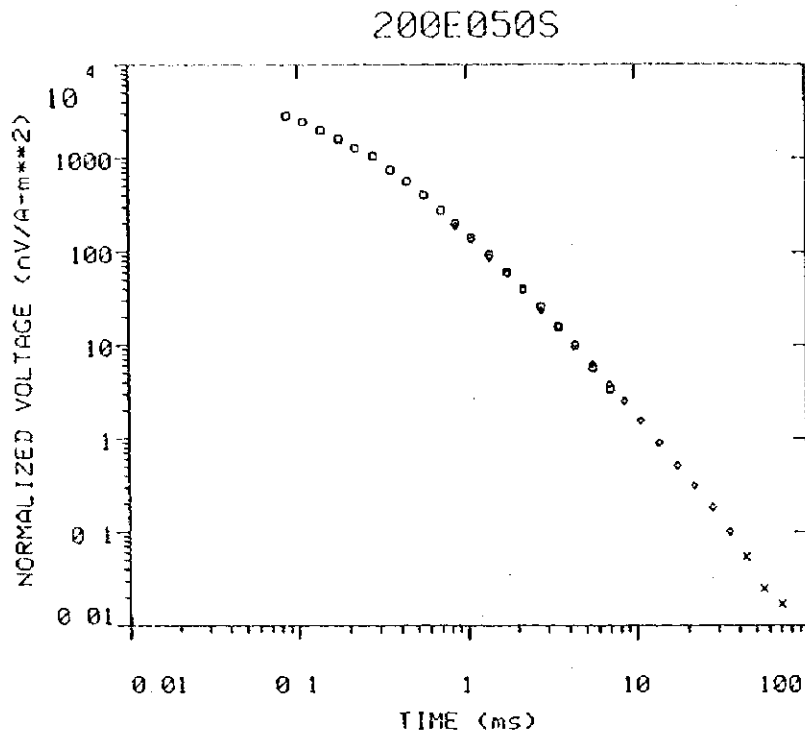


Fig. II -3-2 Example of TEM decay curve

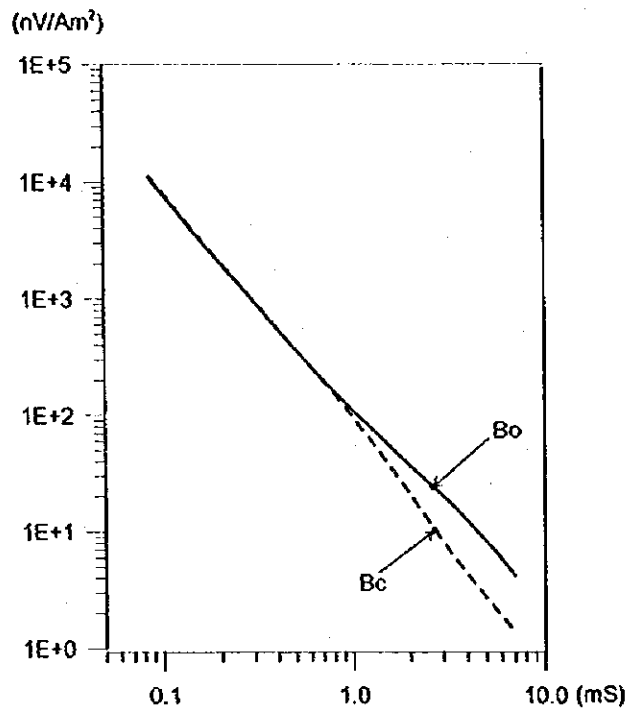


Fig. II -3-3 Observed and background TEM responses

Where ρ is the average resistivity(Ω -m), t is the time(msec) and d is the depth(meter)

3-5 Survey Results

3-5-1 Ghuzayn area

(1) Loop locations

A TEM survey by using large loops was carried out based on the high chargeability anomalies detected on the lines 2400W to 2800W by the TDIP survey as it was mentioned in Chapter 2. A large loop of 600m by 600m was utilized. Fig.II-2-4 illustrates the locations of the large loops.

The estimated depth of investigation of the anomaly sources have been calculated taking into account the formula for exploration depth described in Section 3-4 of this Chapter. Table II-3-4 shows the estimated depth in the large loop No. 1 surveyed in Ghuzayn area as a function of the channel times. Since these values are calculated for a layered resistivity structure at the center of the loop, the calculated depth should be taken with caution because it does not always correspond to the real depth.

Table II-3-4 Depth estimation in survey area

| | | Unit: meter | | | | | | | | | | | | | | |
|---------|------------------|-------------|-------|-------|-------|-------|-------|-------|-------|------------|-------|-------|-------|-------|--|--|
| Channel | Ghuzayn Loop1 | Sarami | | | | | | | | Hara Kilab | | | | | | |
| | | Loop1 | Loop2 | Loop3 | Loop4 | Loop5 | Loop6 | Loop7 | Loop8 | Loop1 | Loop2 | Loop3 | Loop4 | Loop5 | | |
| Ch1 | 40 | 45 | 45 | 56 | 56 | 43 | 39 | 51 | 44 | 32 | 52 | 36 | 38 | 56 | | |
| Ch2 | 44 | 50 | 49 | 62 | 62 | 47 | 43 | 56 | 48 | 35 | 57 | 39 | 42 | 62 | | |
| Ch3 | 49 | 55 | 54 | 68 | 68 | 53 | 48 | 62 | 53 | 39 | 63 | 43 | 47 | 69 | | |
| Ch4 | 55 | 61 | 60 | 76 | 76 | 58 | 53 | 69 | 59 | 43 | 70 | 48 | 52 | 76 | | |
| Ch5 | 61 | 68 | 67 | 84 | 84 | 65 | 59 | 76 | 66 | 48 | 78 | 54 | 58 | 85 | | |
| Ch6 | 68 | 76 | 75 | 94 | 94 | 73 | 66 | 85 | 73 | 53 | 87 | 60 | 65 | 95 | | |
| Ch7 | 76 | 85 | 84 | 106 | 106 | 81 | 74 | 95 | 82 | 60 | 98 | 67 | 73 | 106 | | |
| Ch8 | 85 | 95 | 94 | 119 | 119 | 91 | 83 | 107 | 92 | 67 | 109 | 75 | 82 | 119 | | |
| Ch9 | 96 | 107 | 106 | 133 | 133 | 102 | 93 | 120 | 104 | 75 | 123 | 85 | 92 | 134 | | |
| Ch10 | 108 | 120 | 119 | 150 | 150 | 115 | 105 | 135 | 117 | 85 | 138 | 95 | 103 | 151 | | |
| Ch11 | 121 | 136 | 134 | 168 | 168 | 130 | 118 | 152 | 131 | 95 | 156 | 107 | 116 | 170 | | |
| Ch12 | 137 | 153 | 151 | 190 | 190 | 146 | 133 | 171 | 148 | 107 | 175 | 120 | 131 | 191 | | |
| Ch13 | 154 | 172 | 170 | 214 | 214 | 164 | 150 | 193 | 166 | 121 | 197 | 136 | 147 | 215 | | |
| Ch14 | 174 | 194 | 192 | 241 | 241 | 185 | 169 | 218 | 188 | 136 | 223 | 153 | 166 | 243 | | |
| Ch15 | 196 | 219 | 216 | 272 | 272 | 209 | 191 | 246 | 212 | 154 | 251 | 173 | 187 | 274 | | |
| Ch16 | 221 | 247 | 244 | 307 | 307 | 236 | 215 | 277 | 239 | 173 | 283 | 195 | 211 | 309 | | |
| Ch17 | 249 | 279 | 275 | 346 | 346 | 266 | 243 | 313 | 269 | 196 | 320 | 220 | 238 | 348 | | |
| Ch18 | 282 | 314 | 311 | 391 | 391 | 300 | 274 | 353 | 304 | 221 | 361 | 248 | 269 | 393 | | |
| Ch19 | 318 | 355 | 351 | 441 | 441 | 339 | 310 | 398 | 343 | 249 | 407 | 280 | 303 | 444 | | |
| Ch20 | 359 | 401 | 396 | 498 | 498 | 383 | 349 | 450 | 387 | 281 | 460 | 316 | 342 | 501 | | |

(2) Results

Loop 1

Fig.II-3-4(1) to Fig.II-3-4(2) show the TEM responses obtained from the Loop1 at different channels, i.e. from channel 1 to channel 20.

High TEM responses were detected in two zones: 1) central part of the loop and 2) upper right of the loop. In the zone 1, TEM anomalies are seen from channels 1 to 3 and since they are of shallow



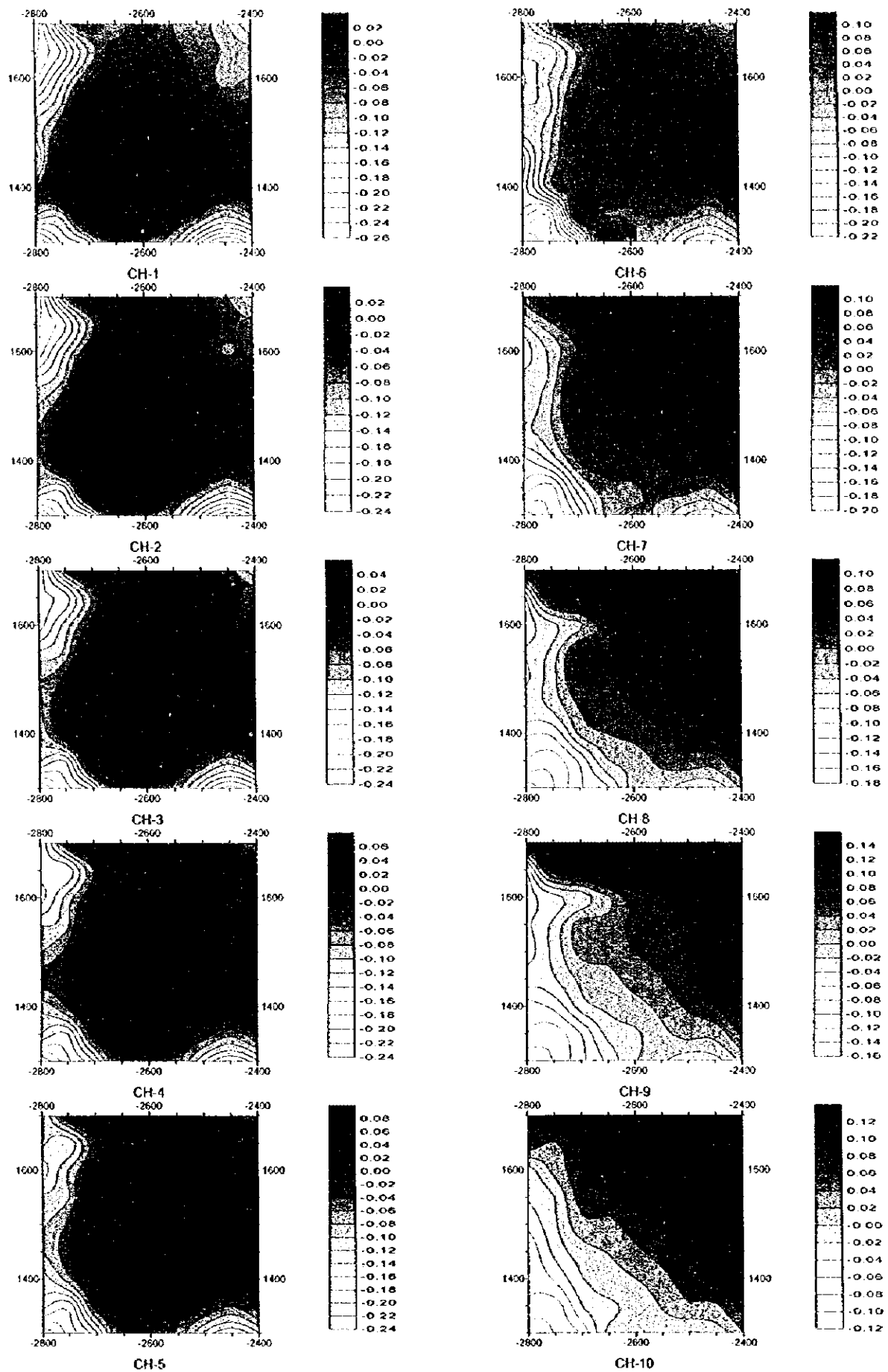


Fig. II -3-4(1) TEM response maps of Loop1 in Ghuzayn area(Ch1-Ch10)



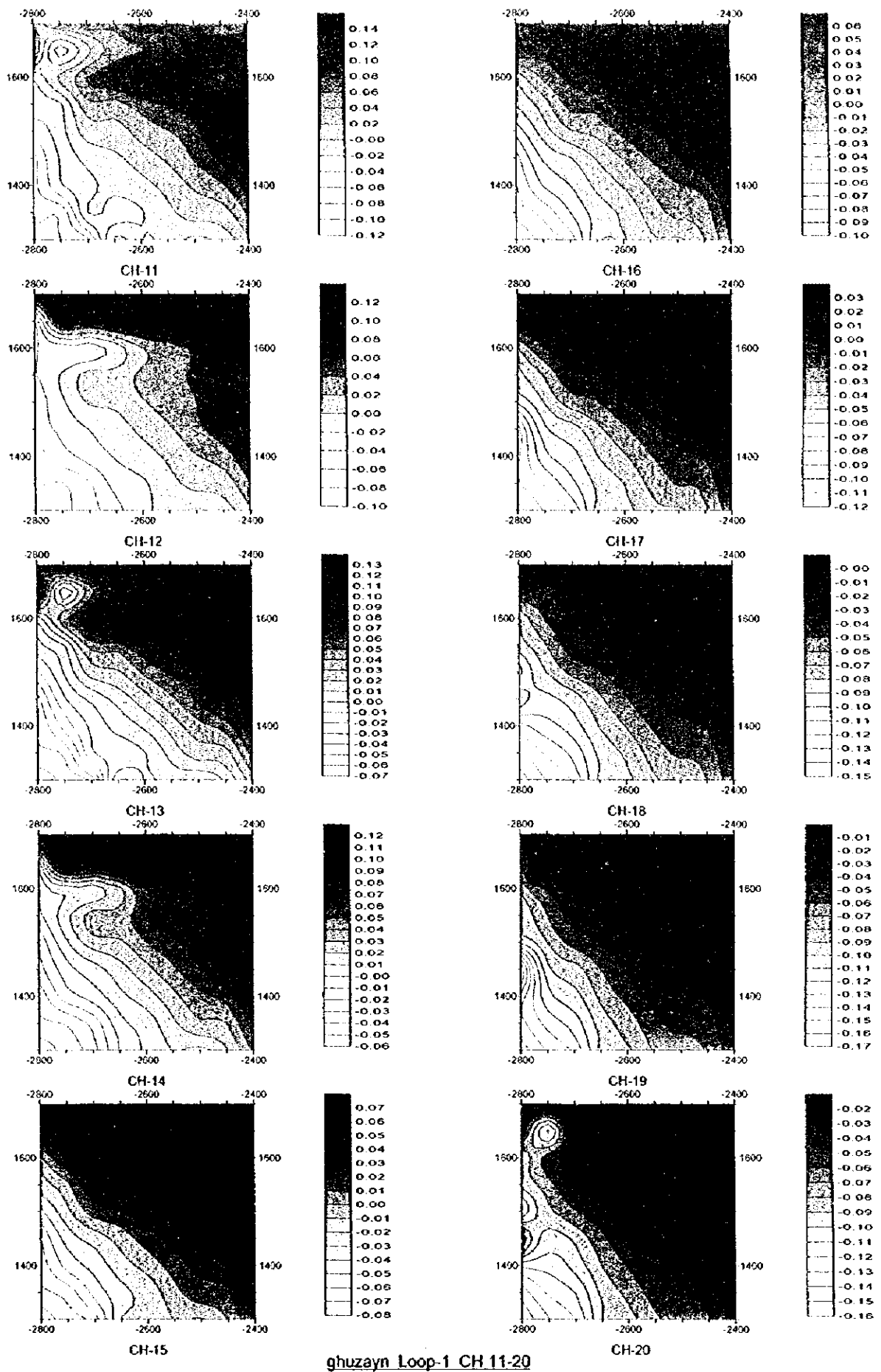


Fig. II-3-4(2) TEM response maps of Loop1 in Ghuzayn area(CH11-Ch20)



nature, they are considered to be the result of underground water. In the zone 2, corresponding to the upper right of the loop, TEM anomalies are detected from channel 9. The anomaly seems to gradually increase from lower left to upper right of the loop and this kind of response is not typical of a massive sulphide ore body. In the upper part of the loop and from left to right, a sharp response is seen in channels 8, 9, 12 and 14 and they are probably due to the effect of the power lines crossing the area. Also in some places are seen small circular anomalies due probably to the effect of power line and not to any underground geological response.

3-5-2 Sarami area

(1) Loops locations

A TEM survey consisting of 8 large fixed loops (Fig.II-2-14) was carried in order to investigate the IP anomalies detected by the TDIP survey carried out during this field season.

(2) Results

Loop 1

Figs.II-3-5(1) and II-3-5(2) show the contour maps of the TEM responses obtained in each of the 20 channels.

Among the channels 5 to 13 a continuous high TEM anomaly is assumed in the central part of the loop. This anomaly corresponds very well with the distinctive high metal factor anomaly detected by the TDIP survey.

To confirm this anomaly, the borehole MJOB-S2 was drilled, but it intersected only pyrite disseminations and veinlets with intense silicification, as described in more detail in Chapter 4 (Section 4-4-2).

Loop 2

Figures II-3-6(1) and II-3-6(2) show the contour maps of the TEM responses for each of the 20 channels. Channels 6 to 12 indicate a continuation of the anomaly detected in the central part of the Loop 1. However, the TEM responses are seen rather weak, for which it can be inferred a very low possibility of detecting massive sulphide ore body in this zone.

Loop 3

Figures II-3-7(1) and II-3-7(2) show the contour maps of the TEM responses for each of the 20 channels. Just to the right of the central part of this loop, high TEM responses were detected between channels 3 to 13 and considered as continuation of the anomaly detected in the Loops 1 and 2.

To confirm this anomaly, the borehole MJOB-S1 was drilled, but it intersected only pyrite disseminations and veinlets in V1-2 and basaltic dikes, as described in more detail in Chapter 4 (Section 4-4-2).



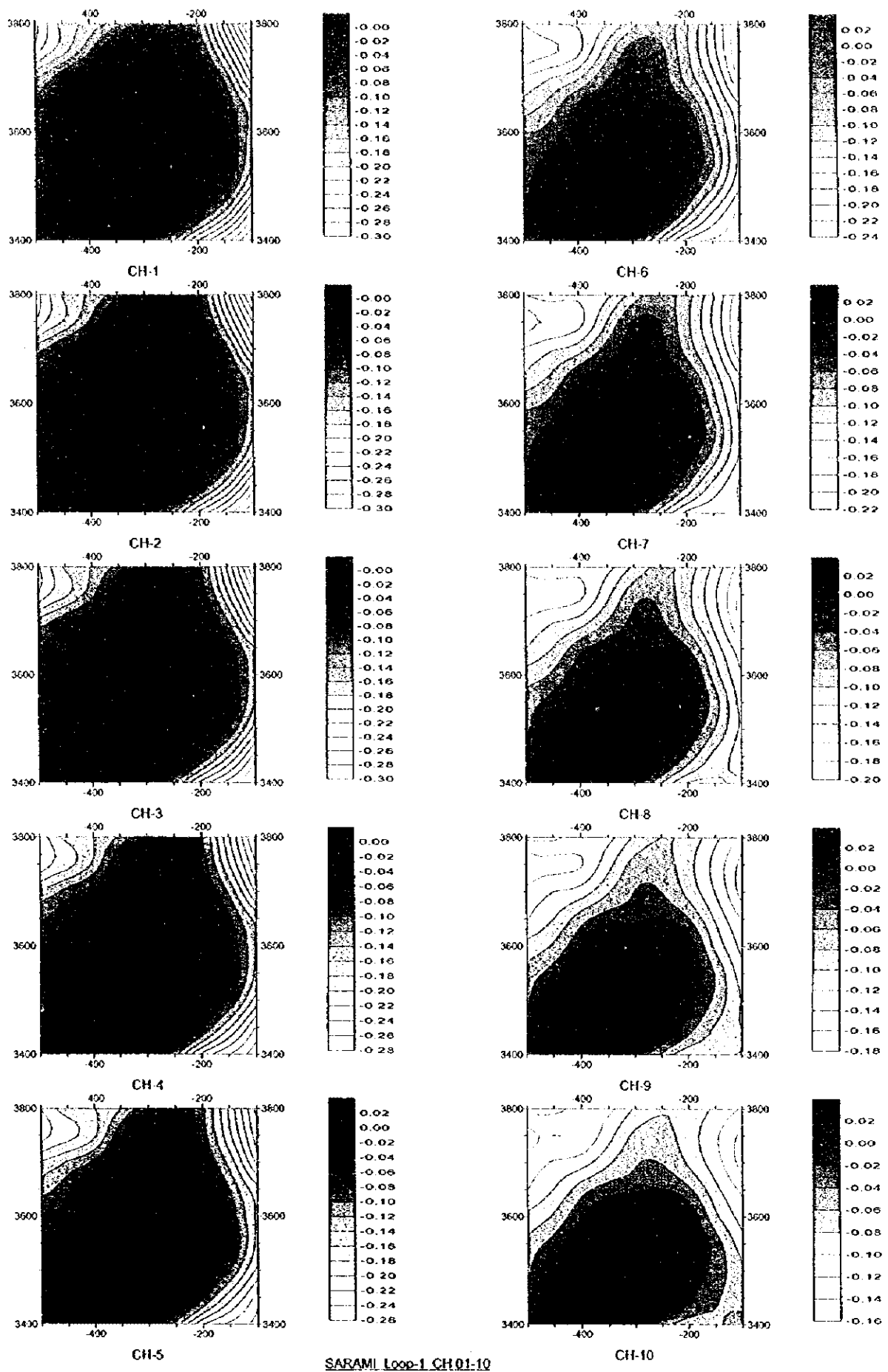


Fig. II-3-5(1) TEM response maps of Loop1 in Sarami area(Ch1-Ch10)

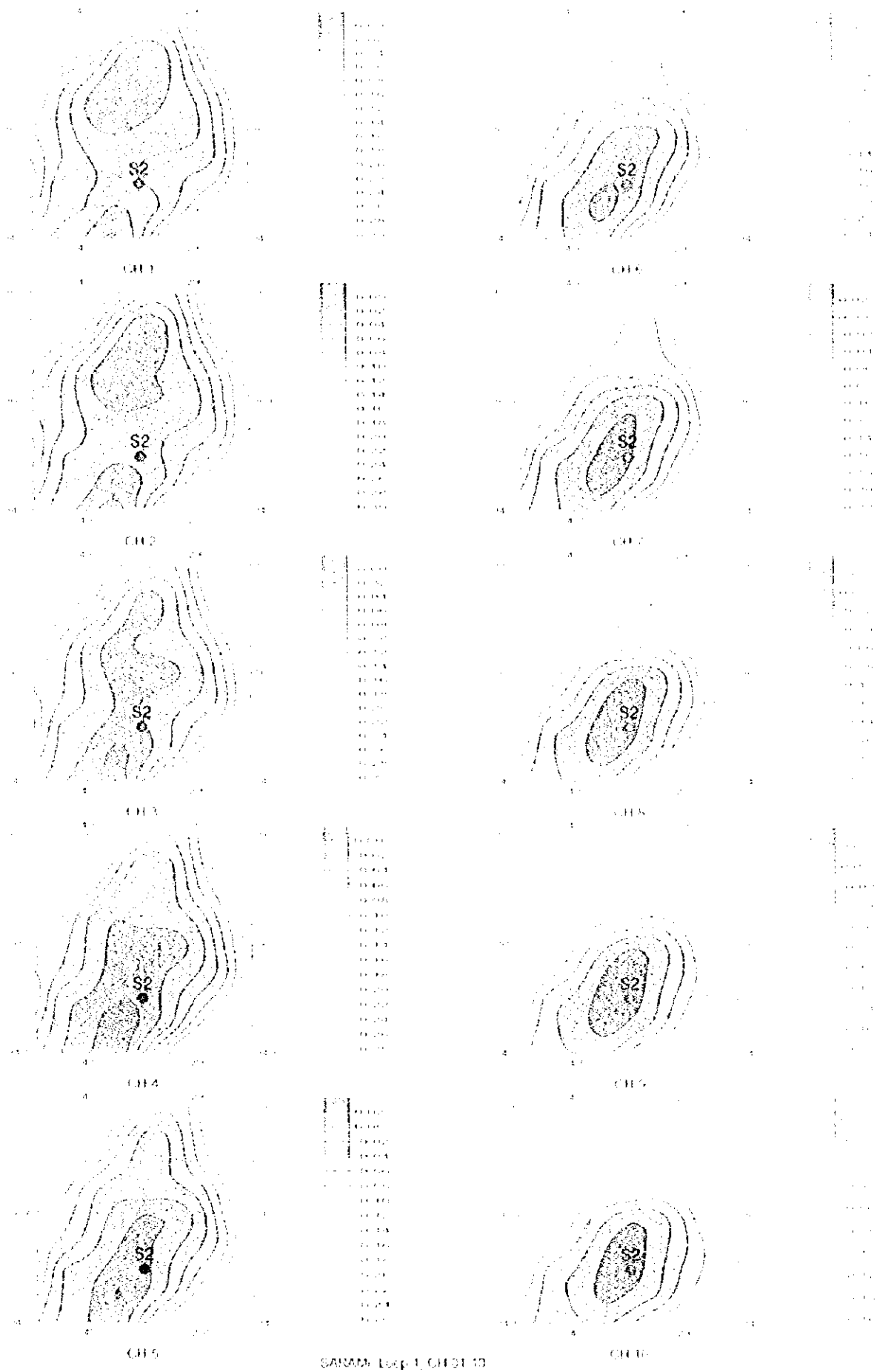


Fig. II-3-5(D) HF M response maps of Loop I in Sarani area (CH1-CH10)



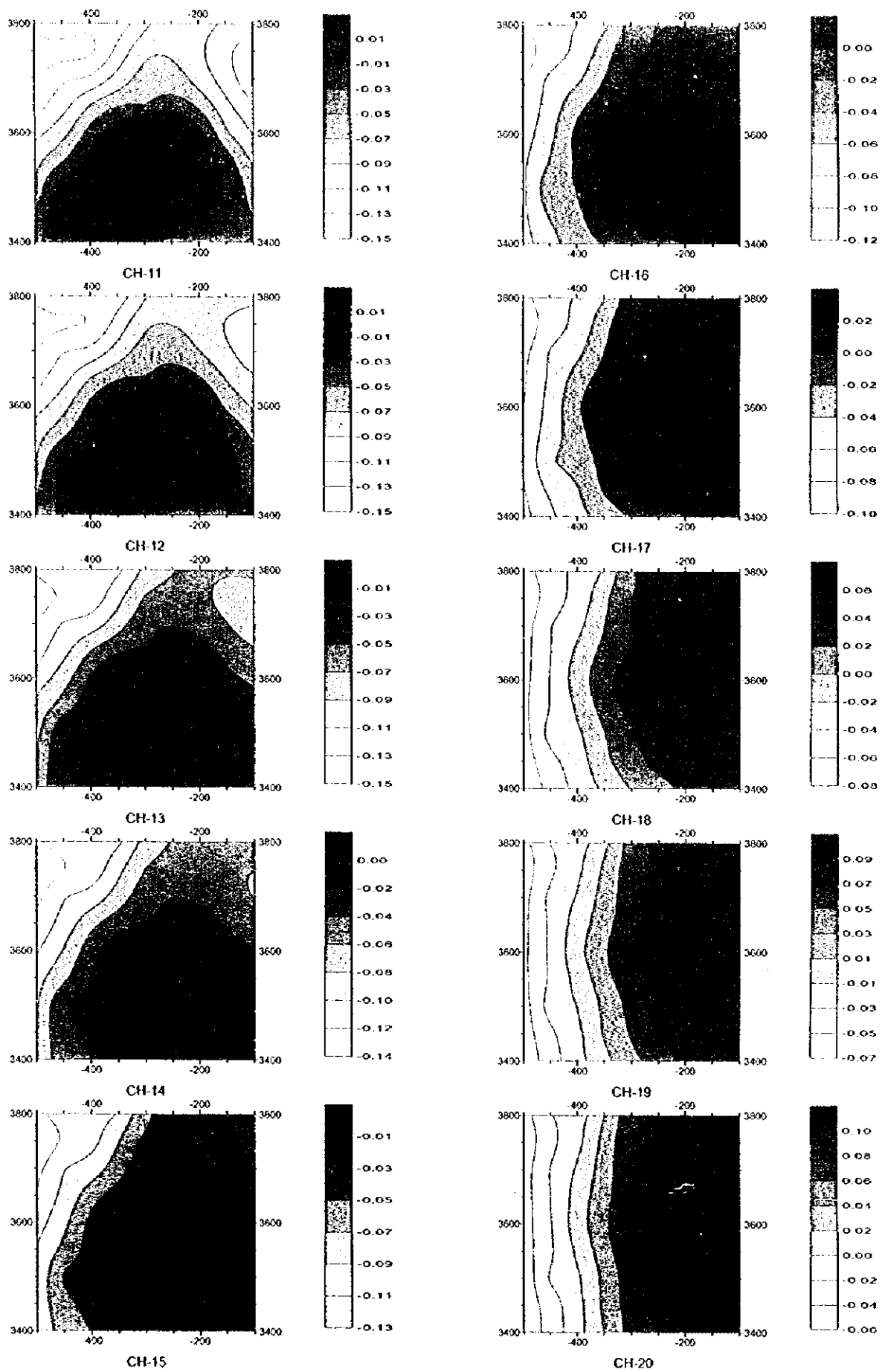


Fig. II-3-5(2) TEM response maps of Loop1 in Sarami area(Ch11-Ch20)

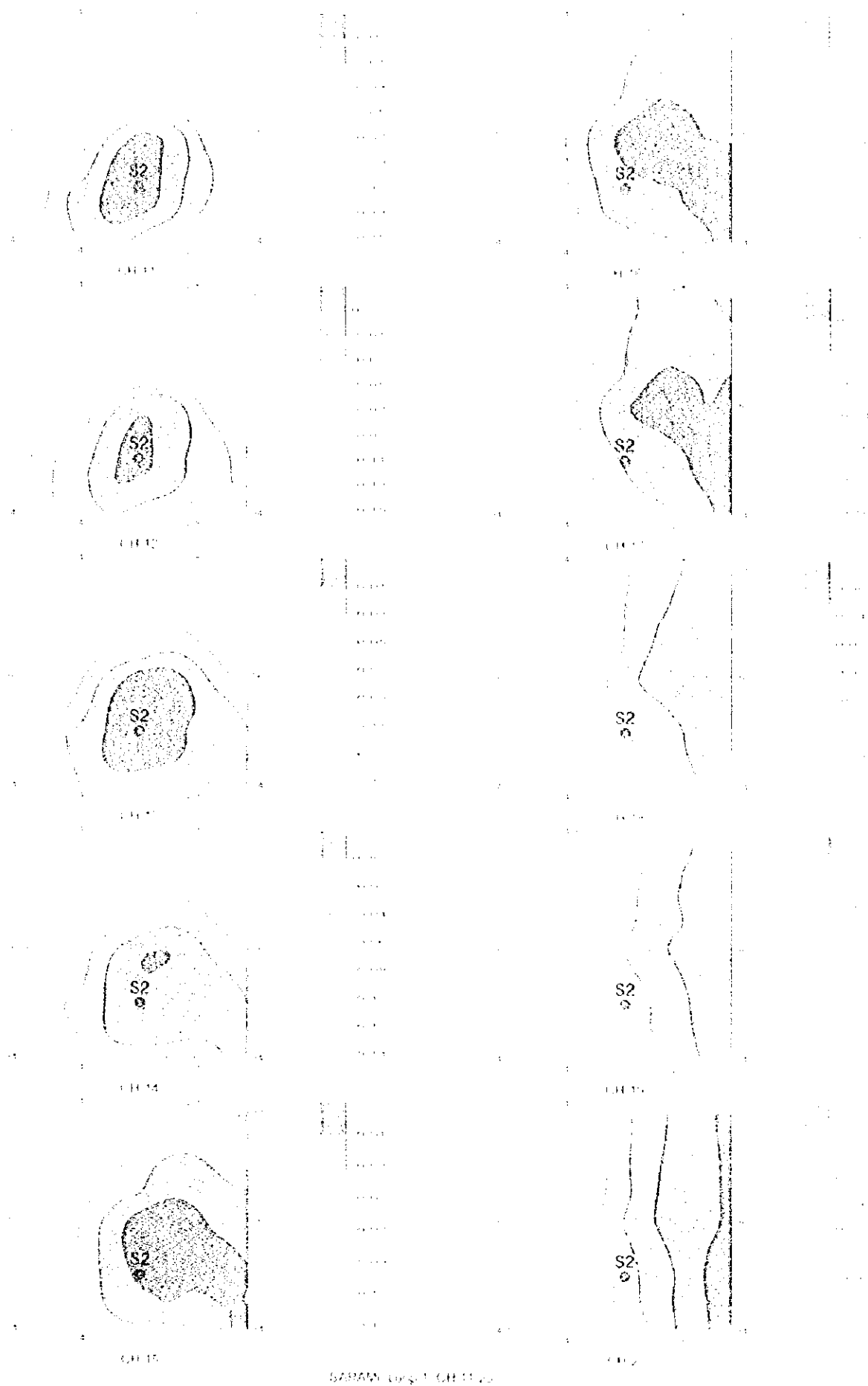


Fig. II-3-5(2) HMI response maps of Loop I in Sagittarius area (CH11-CH20)



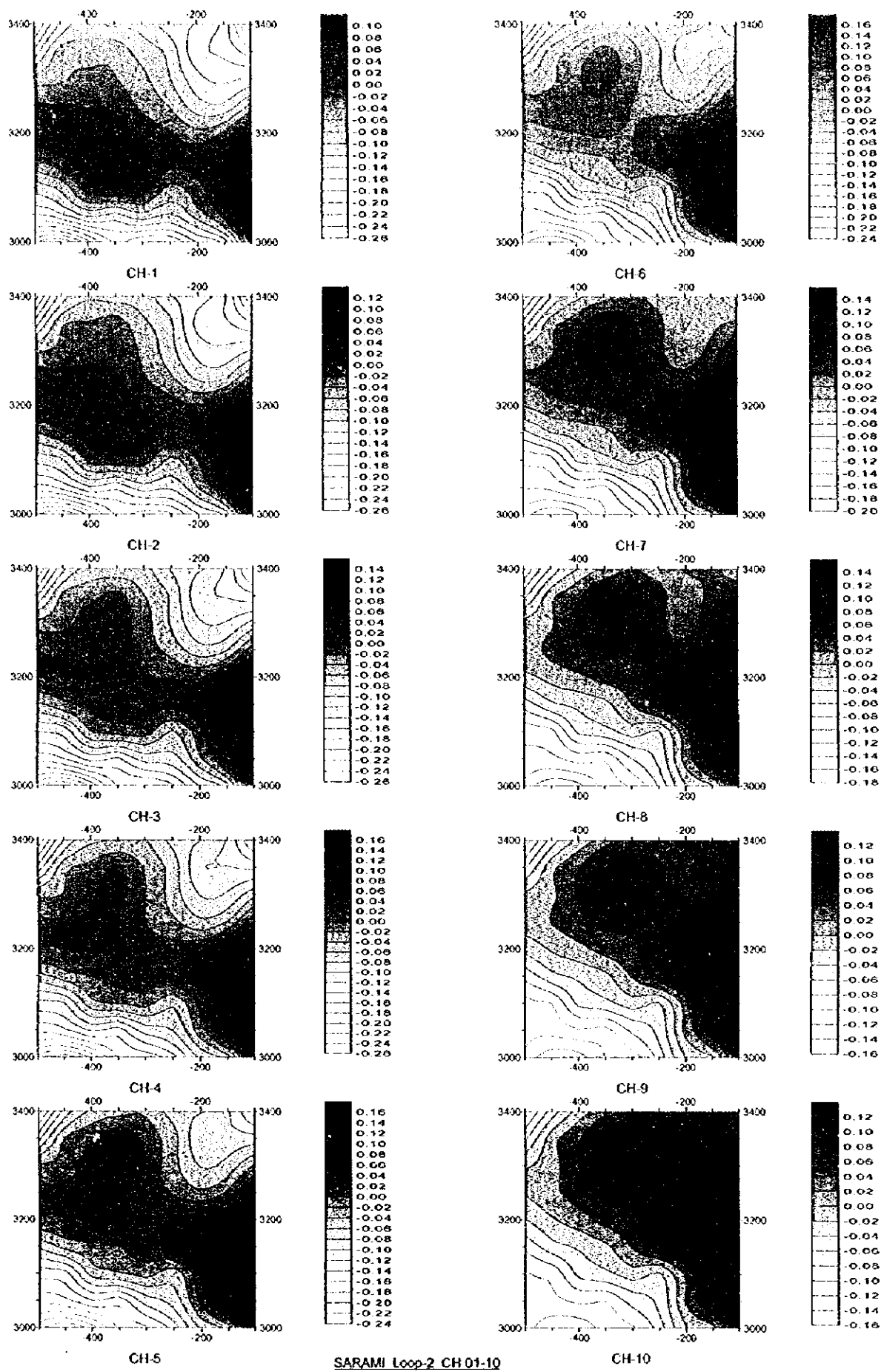


Fig. II-3-6(1) TEM response maps of Loop2 in Sarami area(Ch1-Ch10)



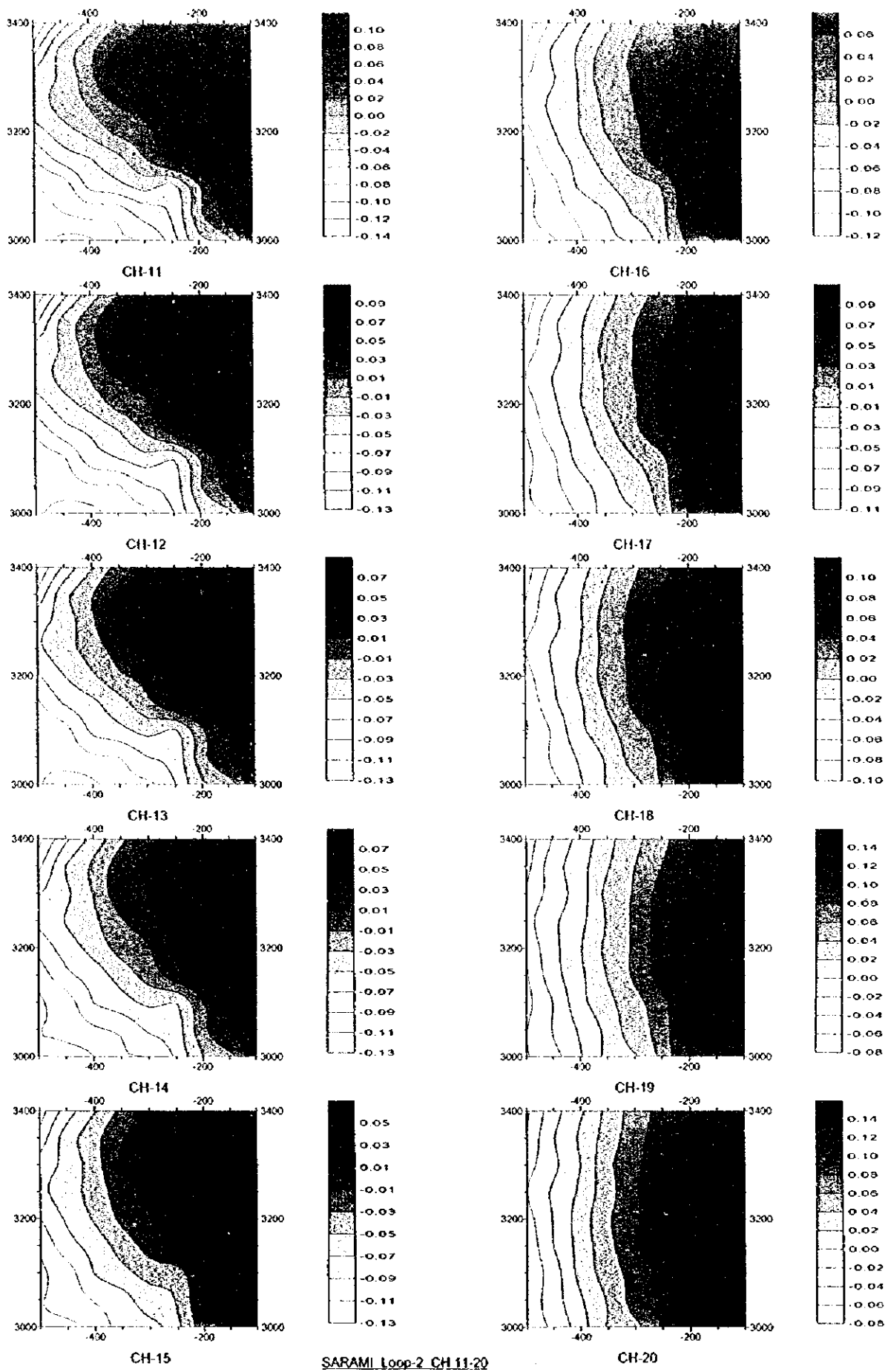


Fig. II-3-6(2) TEM response maps of Loop2 in Sarami area(Ch11-Ch20)



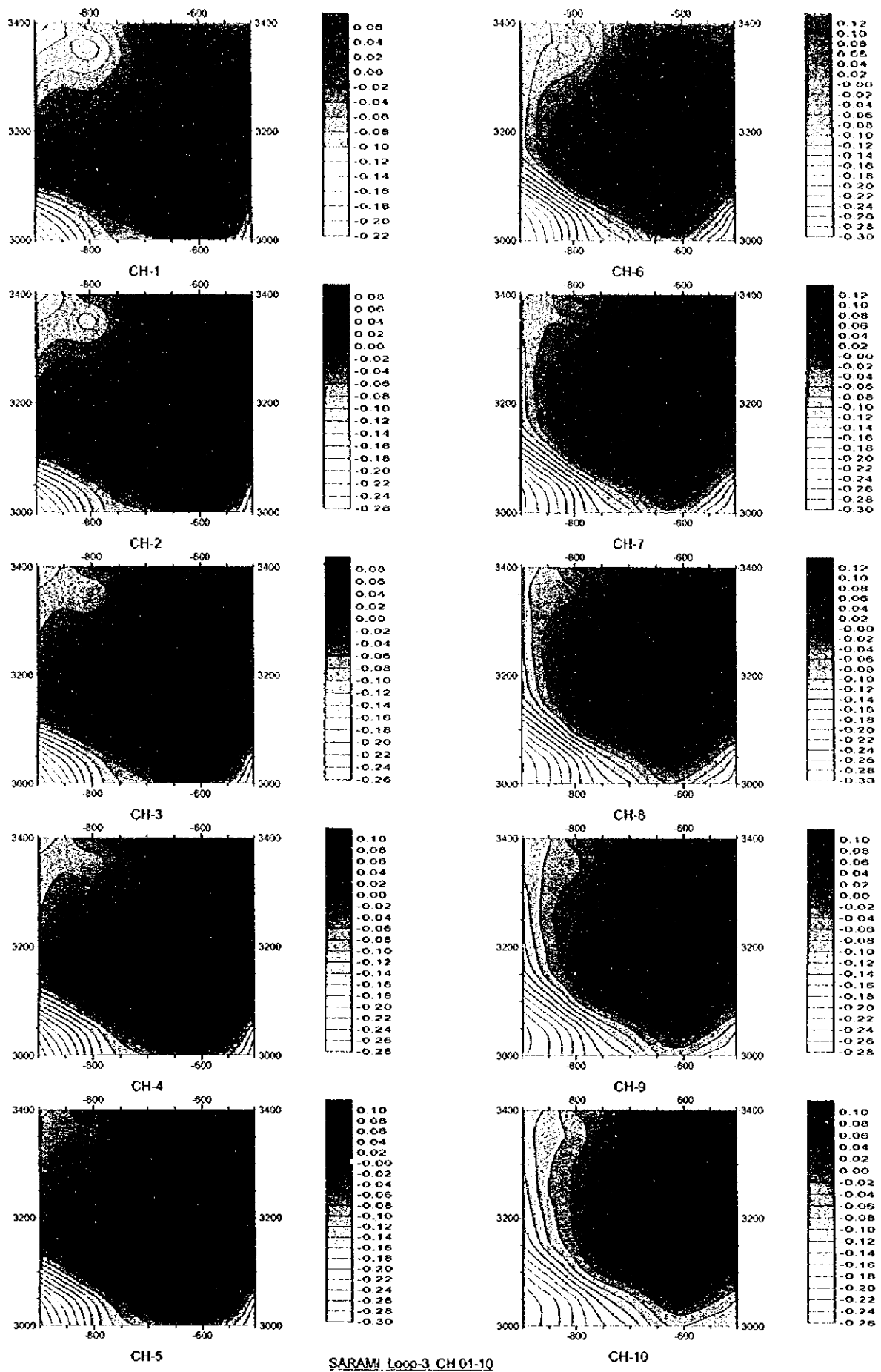


Fig. II -3-7(1) TEM response maps of Loop3 in Sarami area(CH1-Ch10)

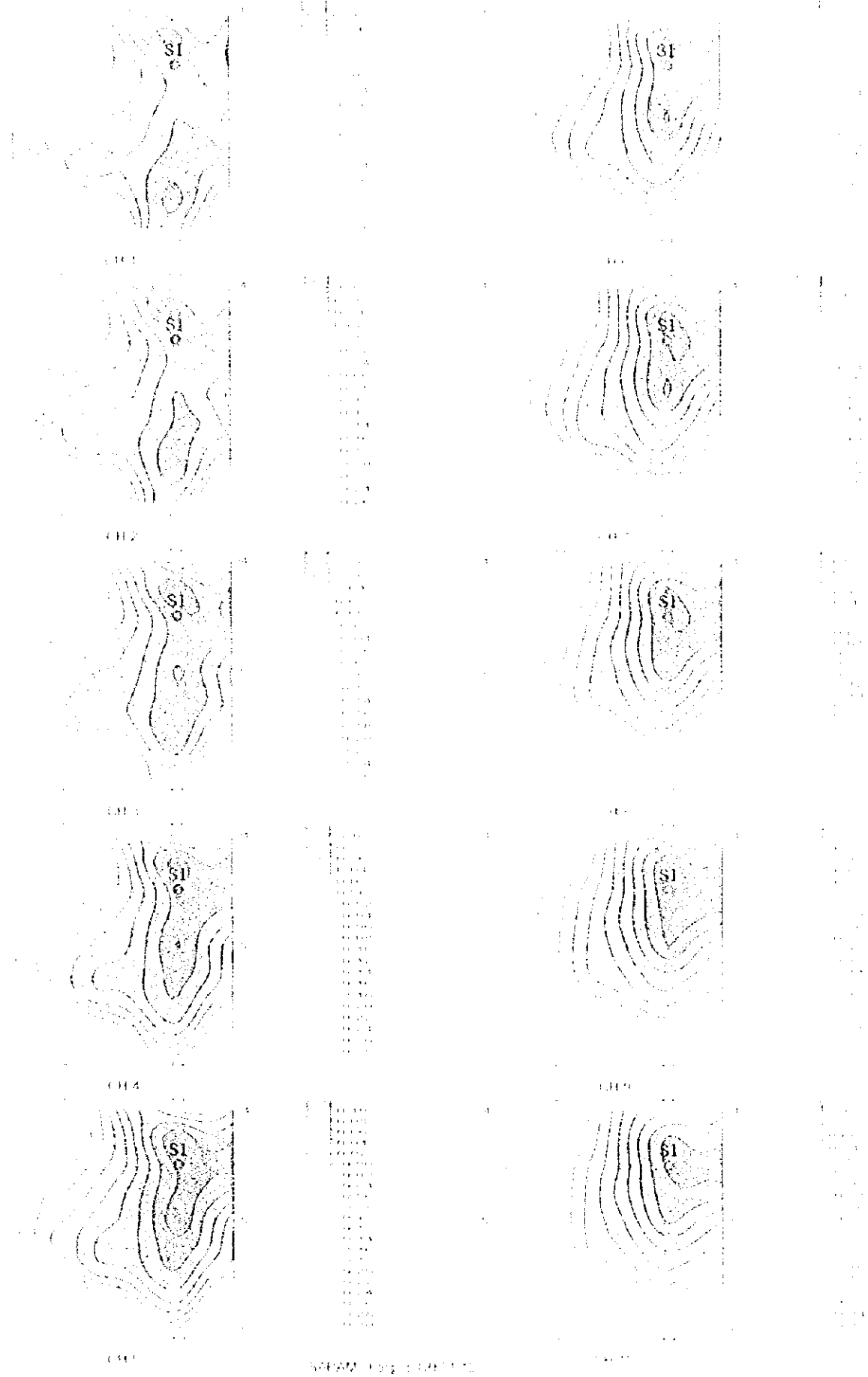


Fig. B-3-115 FEM response maps of Loop 8 in Sarumi area (CH1-CH10)



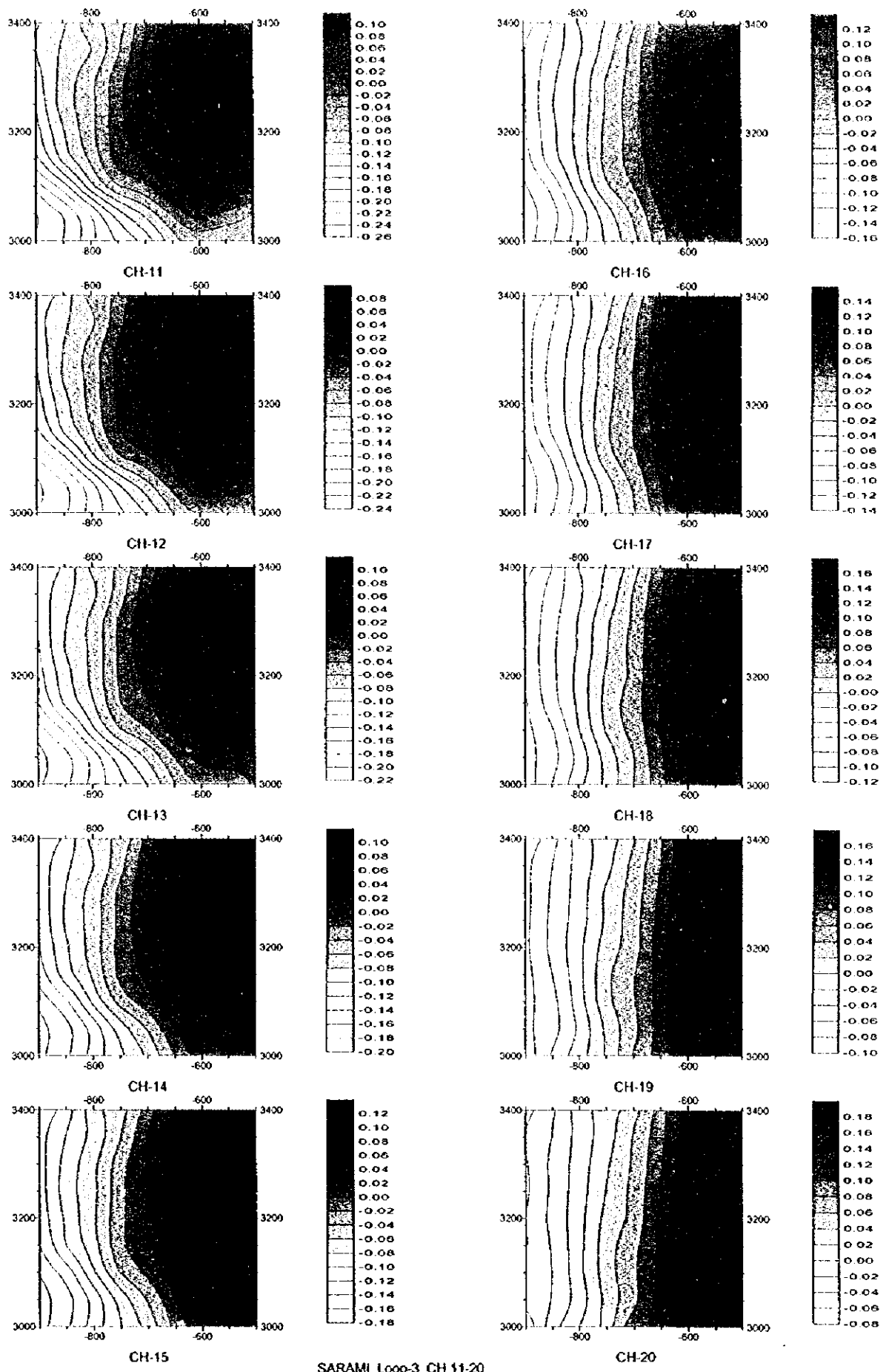


Fig. II-3-7(2) TEM response maps of Loop3 in Sarami area(Ch11-Ch20)

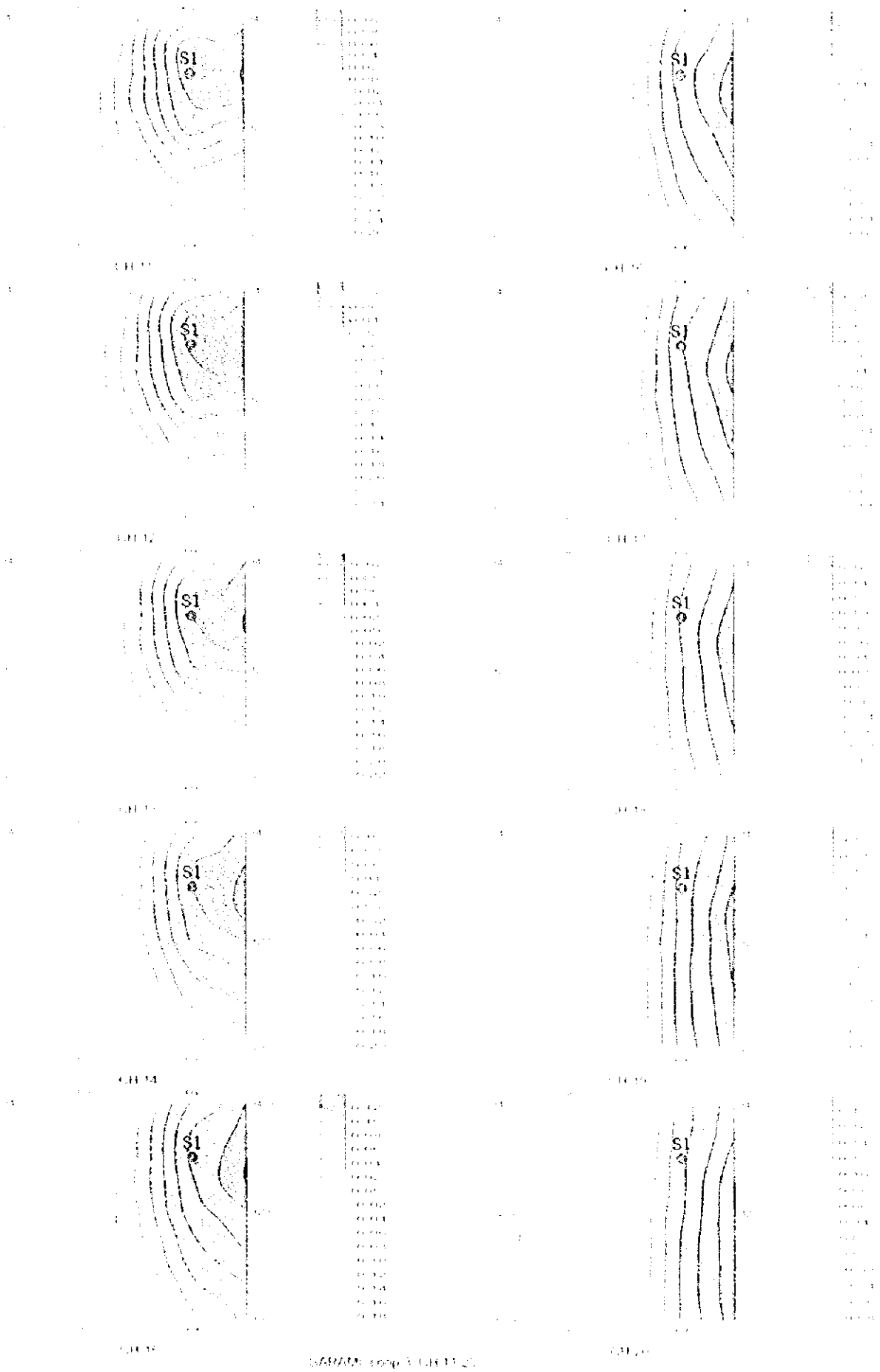


Fig. B-3-7(2) IFM response maps of Loop 3 in Sarani area (Ch 11 - Ch 20)



Loop 4

Figures II-3-8(1) and II-3-8(2) show the contour maps of the TEM responses for each of the 20 channels. In the lower right of this loop, high TEM responses were detected in the channels 1 to 15 and considered as continuation of the anomaly detected in the loop 1, however, the intensity of the TEM response is weak in general.

Loop 5

Figures II-3-9(1) and II-3-9(2) show the contour maps of the TEM responses for each of the 20 channels. Two high TEM responses are seen in this loop: 1) right part of the loop, and 2) lower part of the loop. The anomaly detected in 1) show an elongated pattern along an up-down direction as seen from the channels 1 to 10. This anomaly is very likely due to fracture zones associated to faults. The anomaly detected in 2) is seen from the channels 11 to 15. A fracture zone is probably associated with mineralization, because the boundary between the high and the low chargeability zone is located in this anomaly.

Loop 6

Figures II-3-10(1) and II-3-10(2) show the contour maps of the TEM responses for each of the 20 channels. Excepting for the upper left, high TEM responses are seen almost entirely distributed, which indicate the low resistivity distribution. The high TEM responses correspond to the low chargeability values detected by the TDIP survey and therefore, it is considered that the high TEM responses are not related to mineralization.

Loop 7

Figures II-3-11(1) and II-3-11(2) show the contour maps of the TEM responses for each of the 20 channels. Excepting for the surface, the right side show a gradually increase to high TEM responses, however no distinctive anomaly can be seen.

Loop 8

Figures II-3-12(1) and II-3-12(2) show the contour maps of the TEM responses for each of the 20 channels. Two high TEM responses are seen in this loop: 1) left side of the loop, and 2) right side of the loop. The anomaly detected in 1) are seen from the channels 1 to 8, however it is very likely to be due to a fault seen in this zone. The anomaly detected in 2) is seen in all the channels showing a somewhat gradually increase to high TEM responses. This anomaly may indicate the existence of sulphide mineralization. TEM responses crossing boreholes are shown in Fig II-3-13.

3-5-3 Hara Kilab area

(1) Loop locations

TEM survey was carried to check the IP anomalies detected in the central part of Hara Kilab area



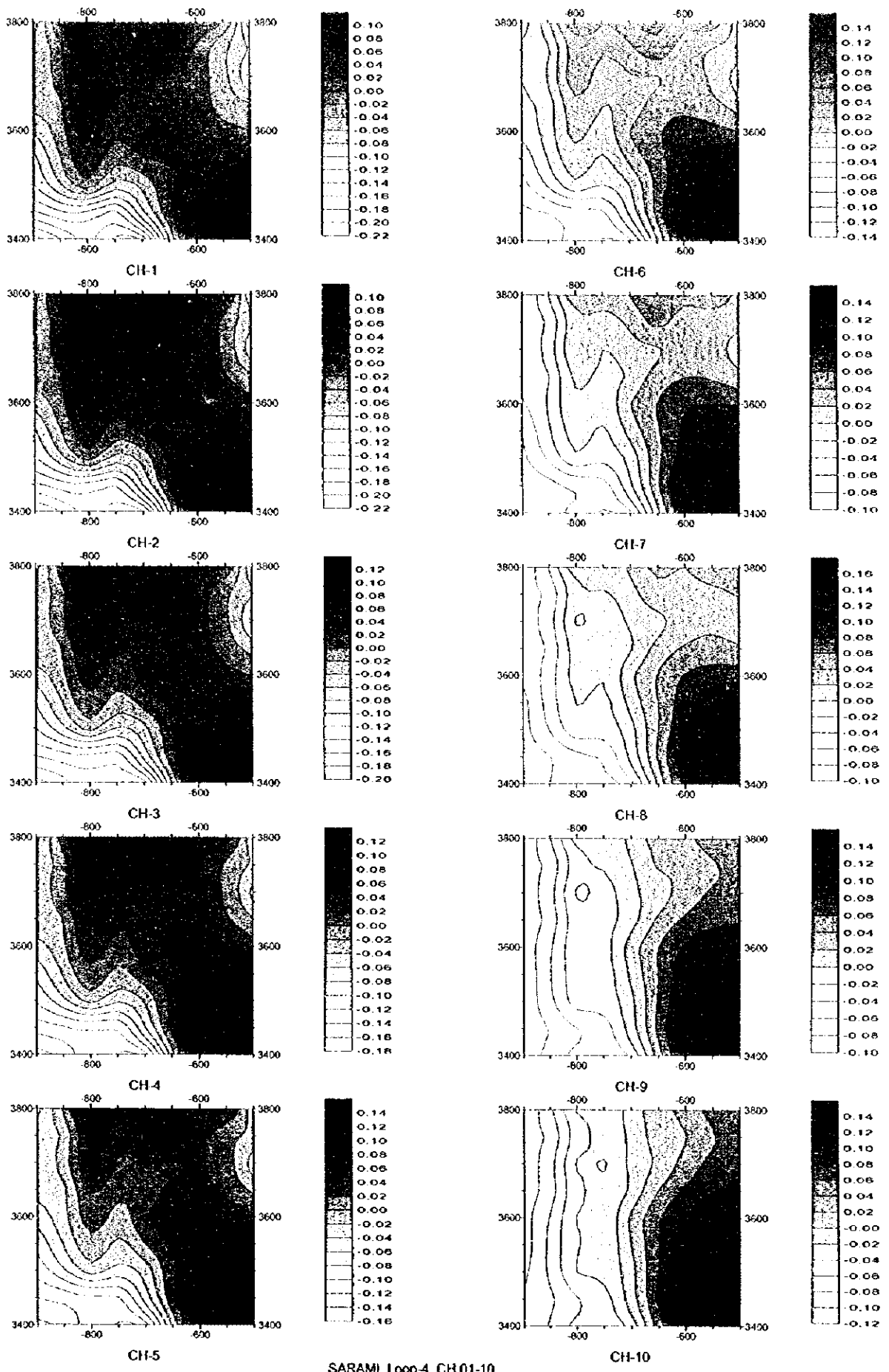


Fig. II-3-8(1) TEM response maps of Loop4 in Sarami area(Ch1-Ch10)



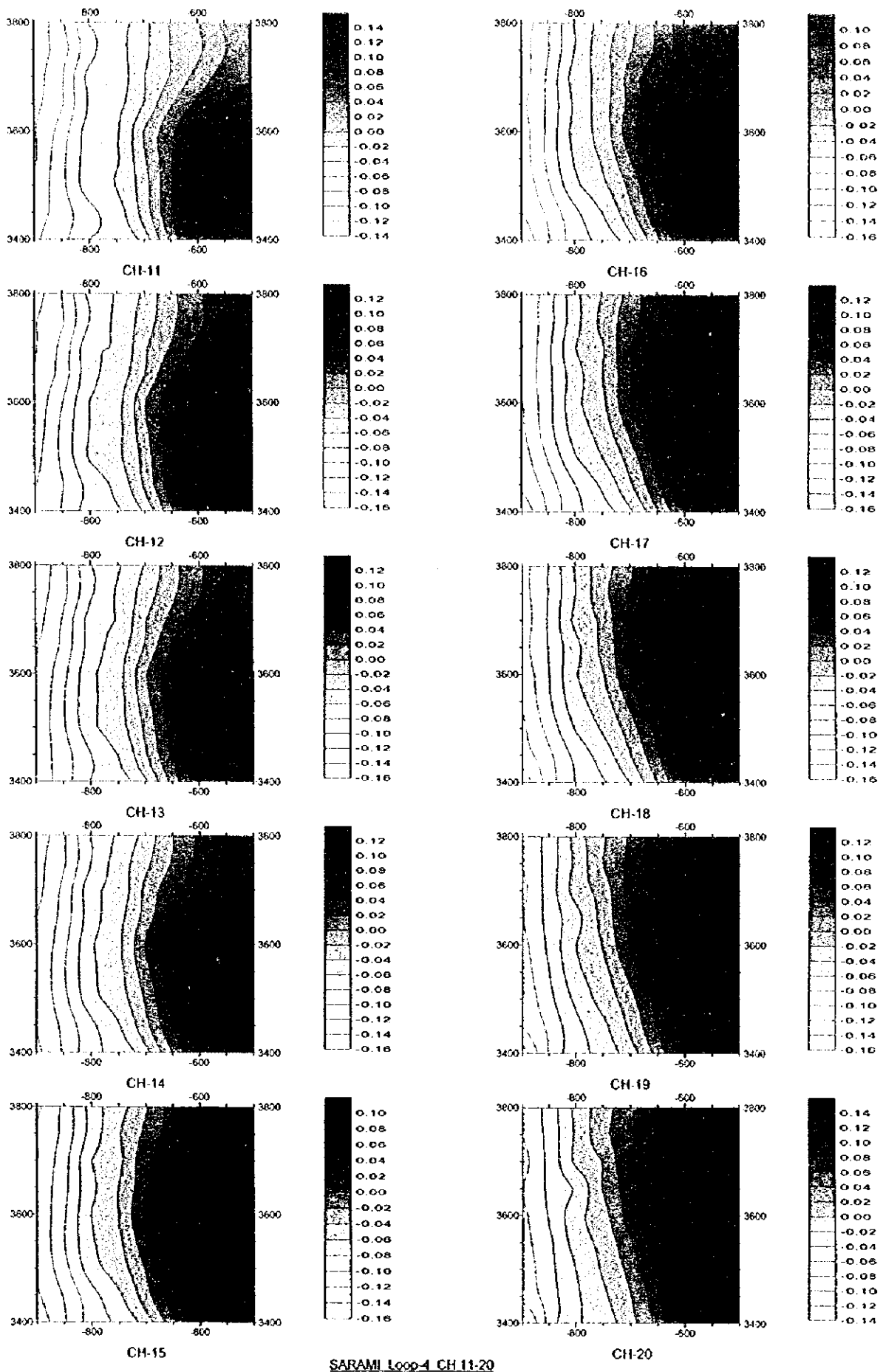


Fig. II-3-8(2) TEM response maps of Loop4 in Sarami area(Ch11-Ch20)



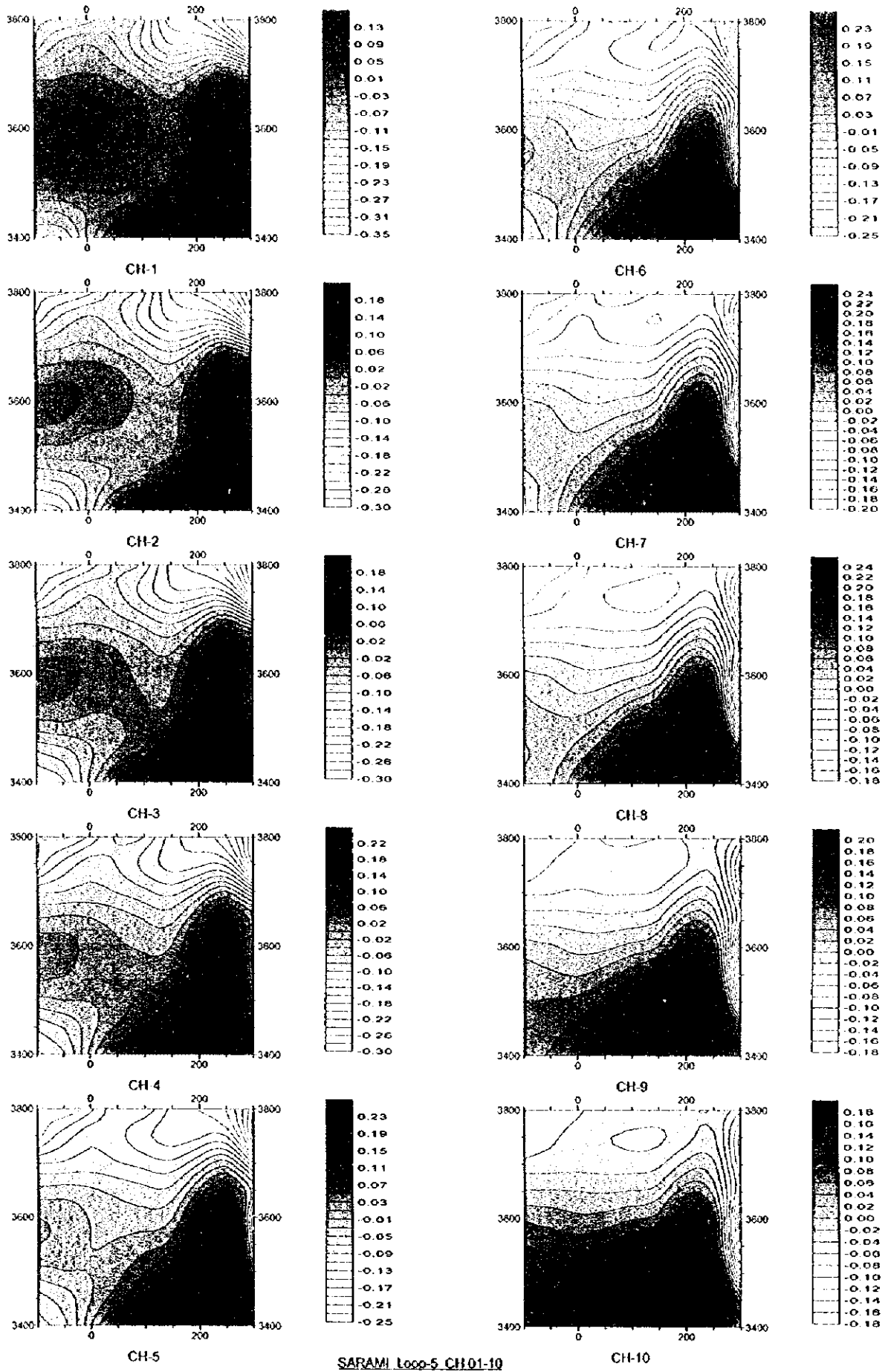


Fig. II-3-9(1) TEM response maps of Loop5 in Sarami area(CH1-CH10)



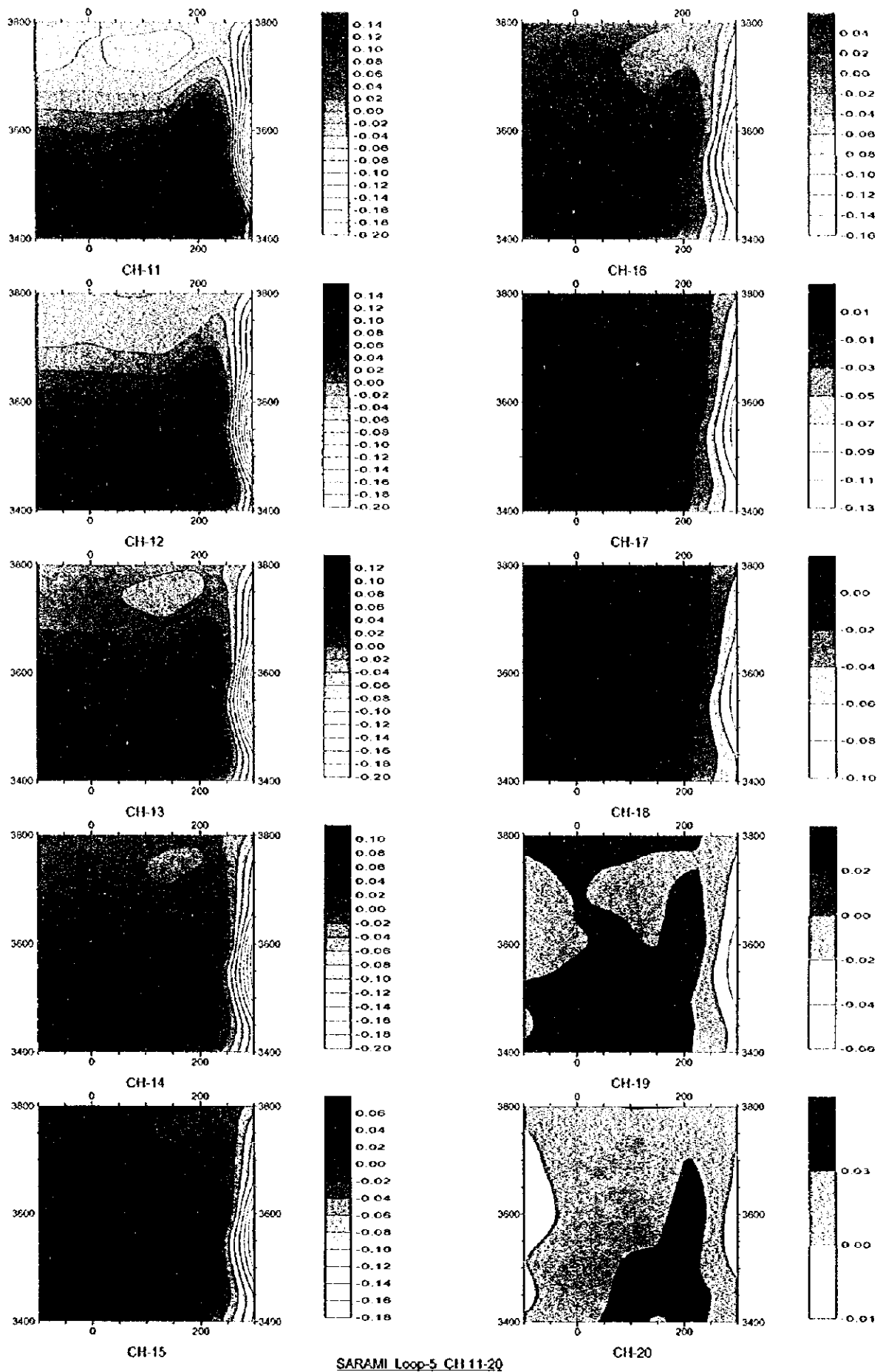
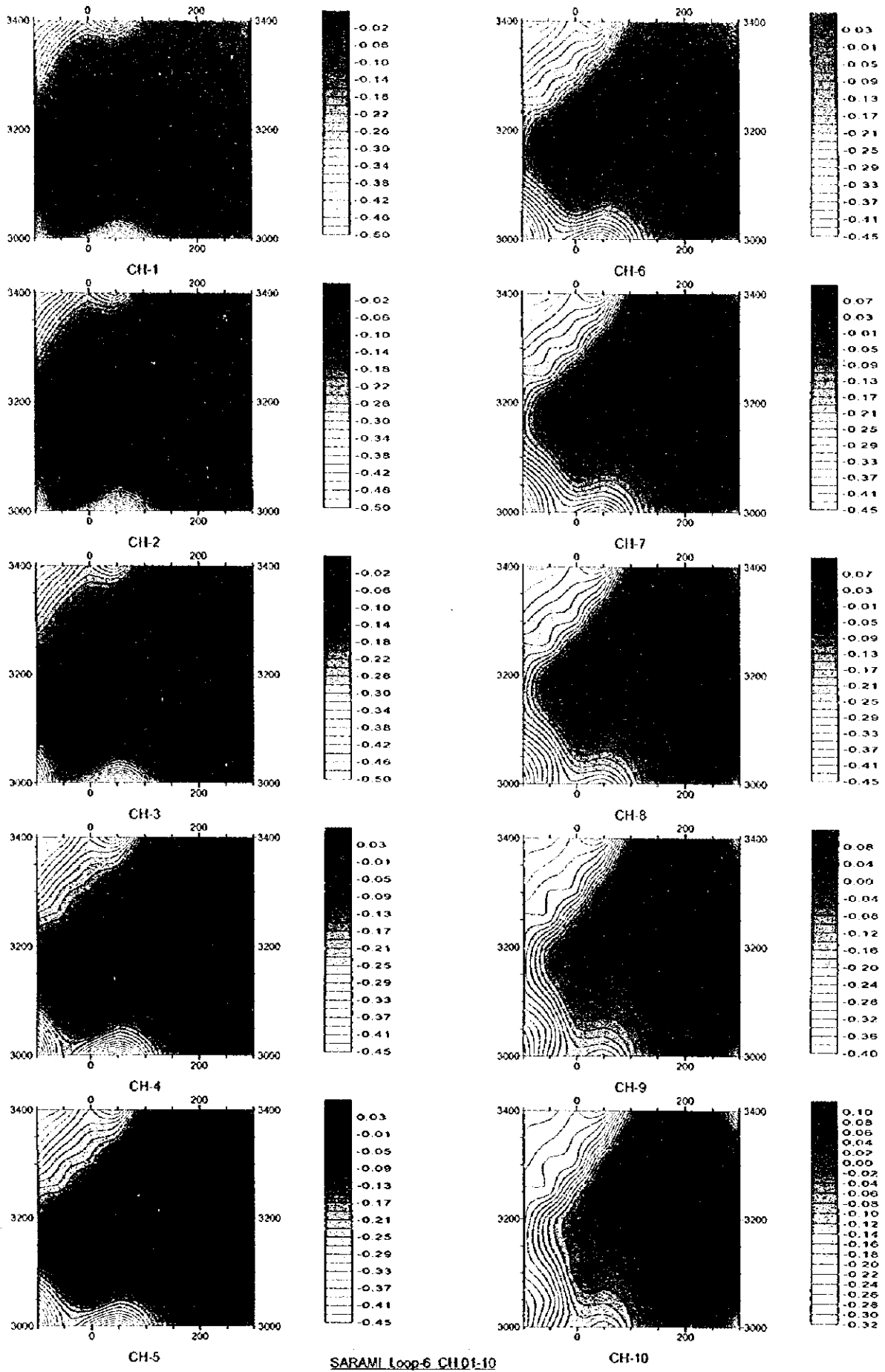


Fig. II-3-9(2) TEM response maps of Loop5 in Sarami area(Ch11-Ch20)





SARAMI Loop-6 CH101-10

Fig. II -3-10(1) TEM response maps of Loop6 in Sarami area(Ch1-Ch10)



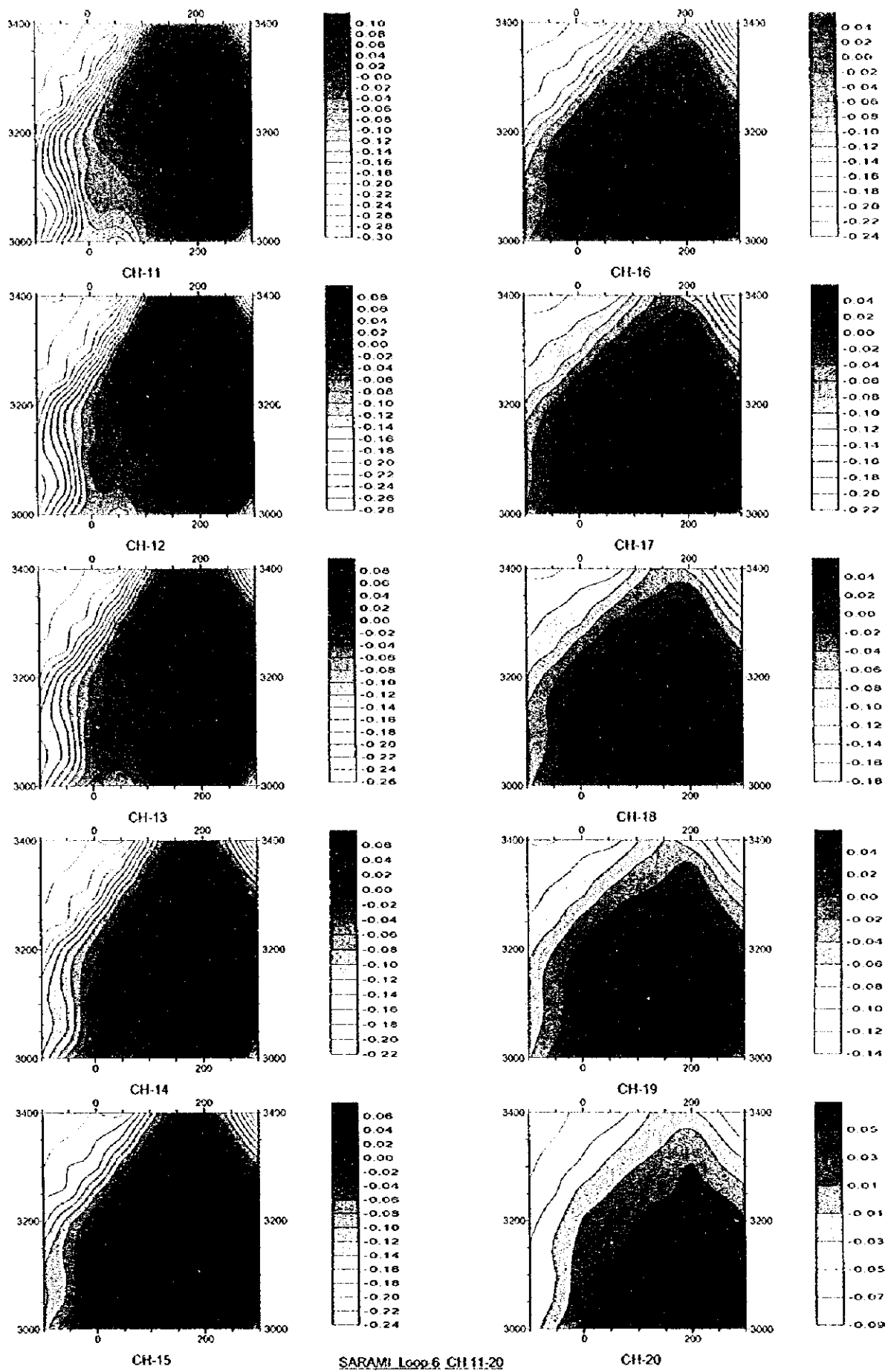


Fig. II-3-10(2) TEM response maps of Loop6 in Sarami area(CH11-CH20)



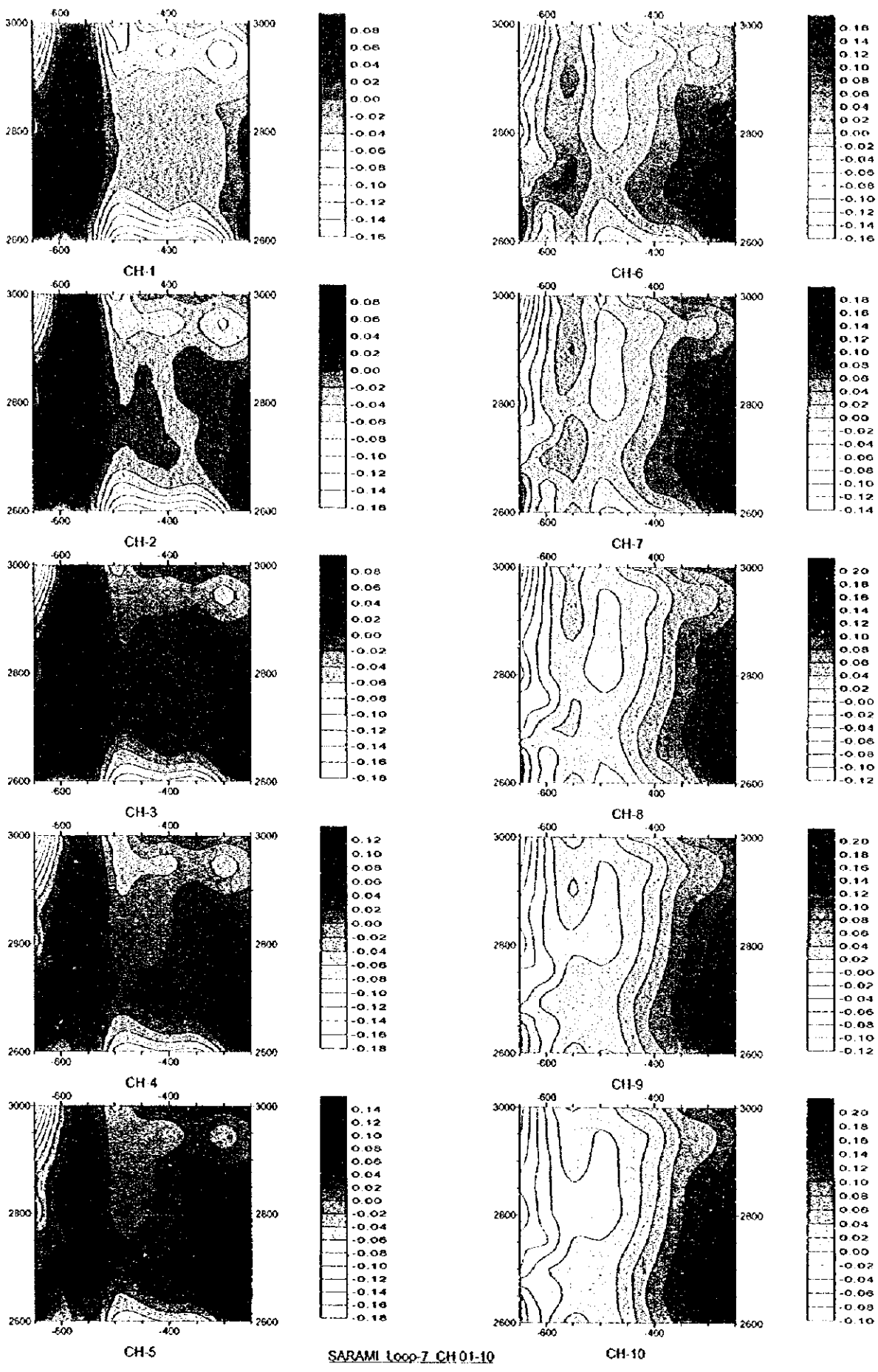
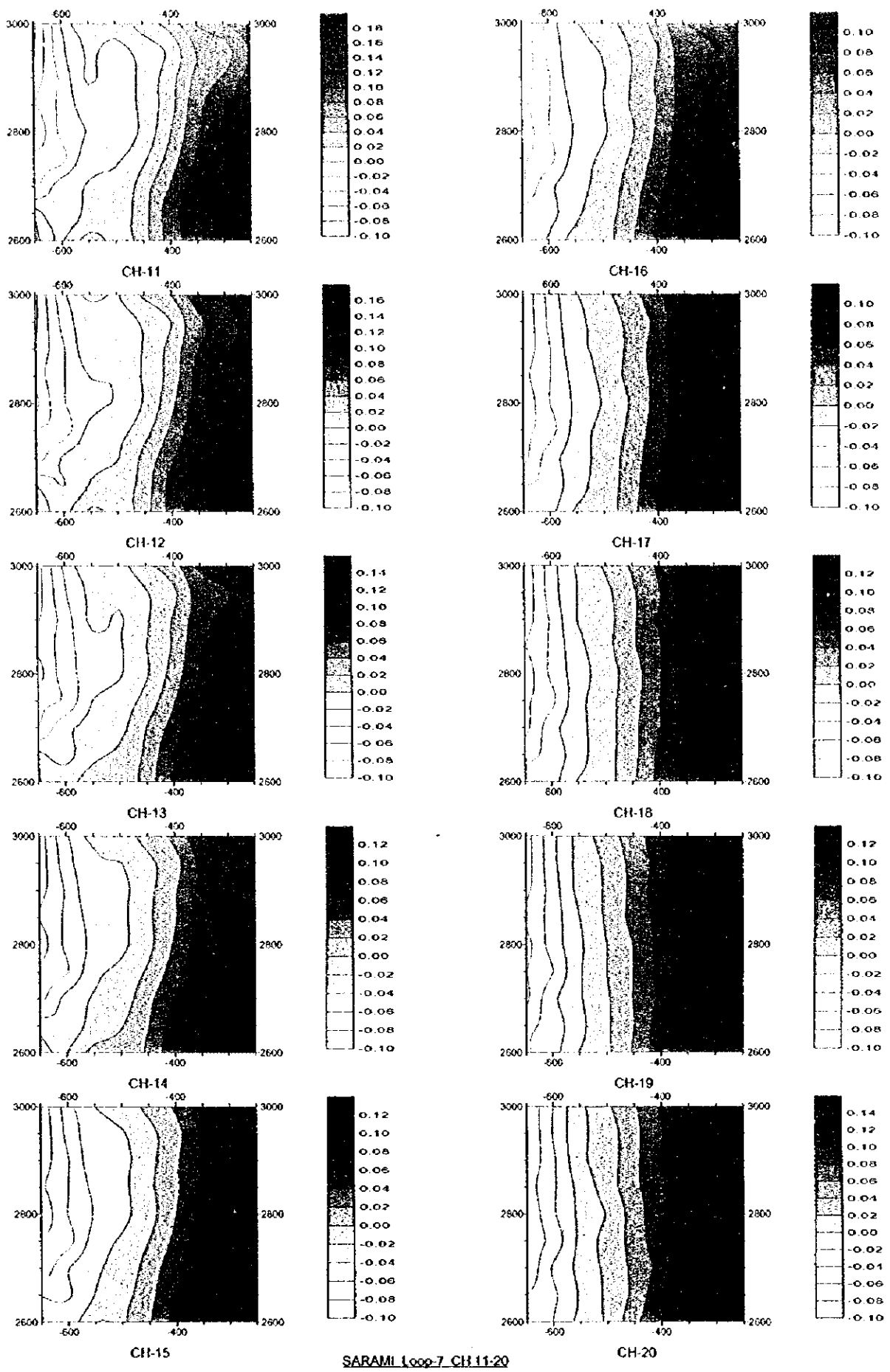


Fig. II-3-11(1) TEM response maps of Loop7 in Sarami area(Ch1-Ch10)





SARAMI Loop-7 CH-11-20

Fig. II-3-11(2) TEM response maps of Loop7 in Sarami area(CH11-CH20)



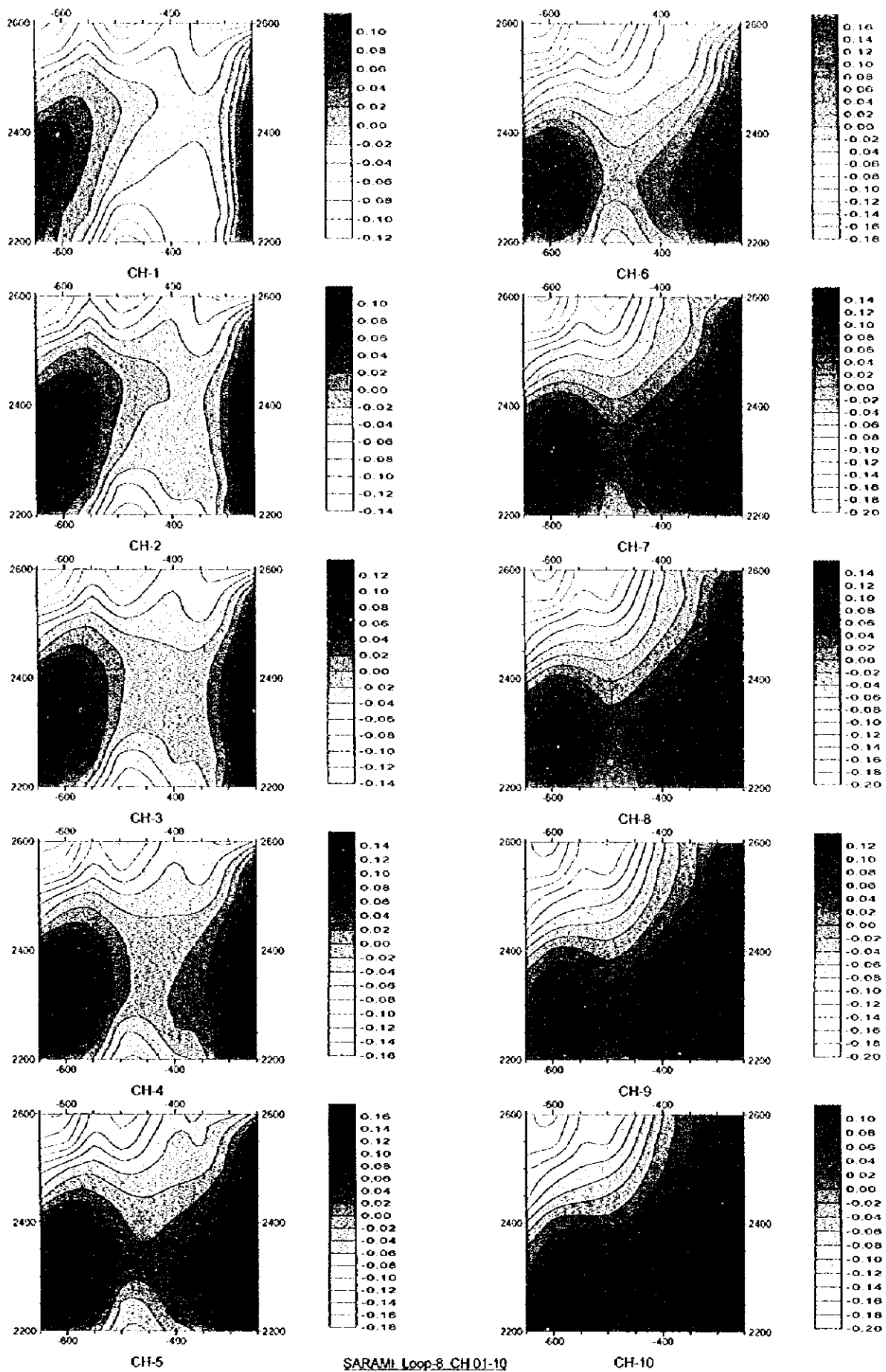


Fig. II-3-12(1) TEM response maps of Loop8 in Sarami area(CH1-Ch10)



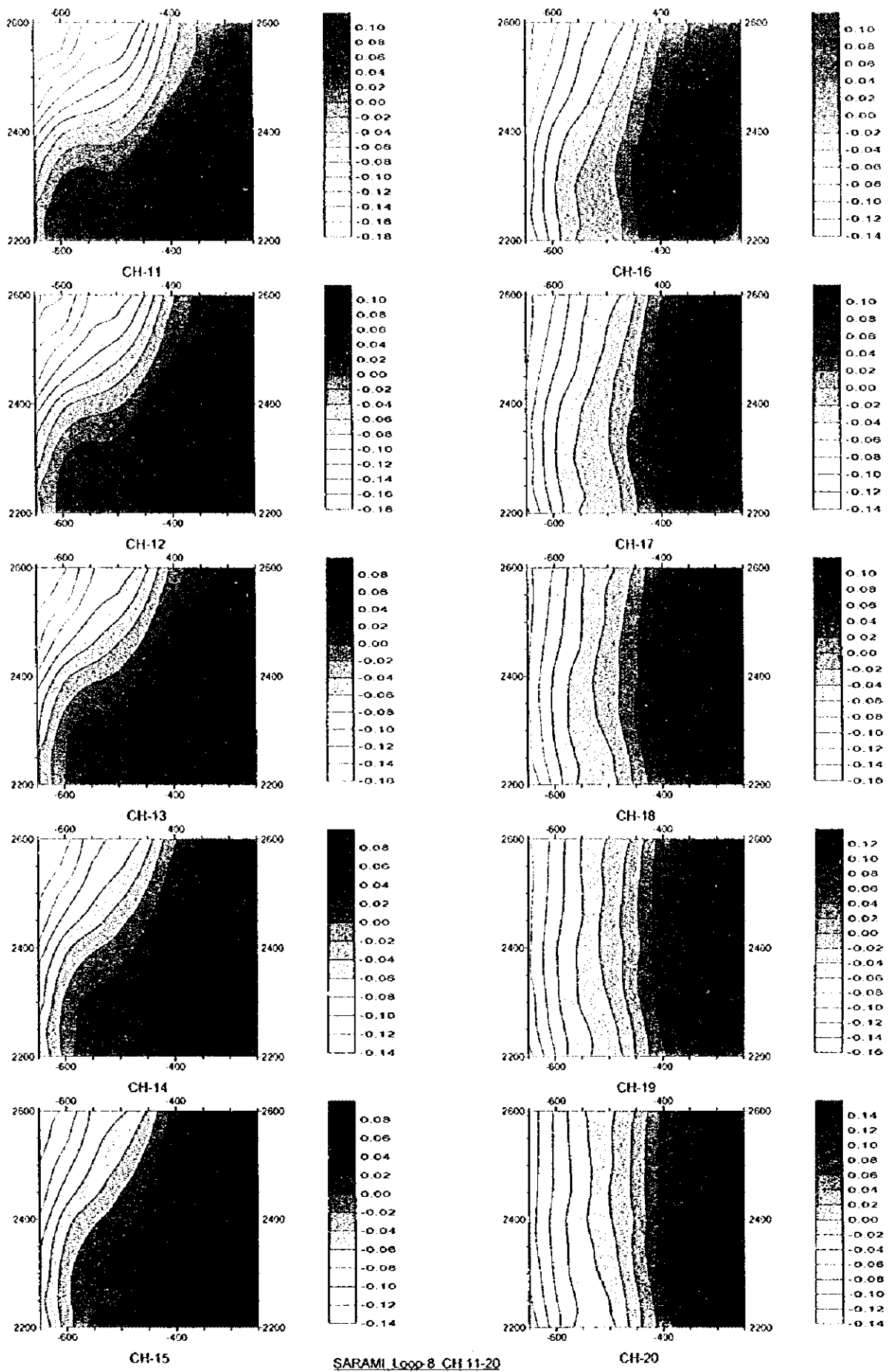


Fig. II-3-12(2) TEM response maps of Loop 8 in Sarami area (Ch11-Ch20)



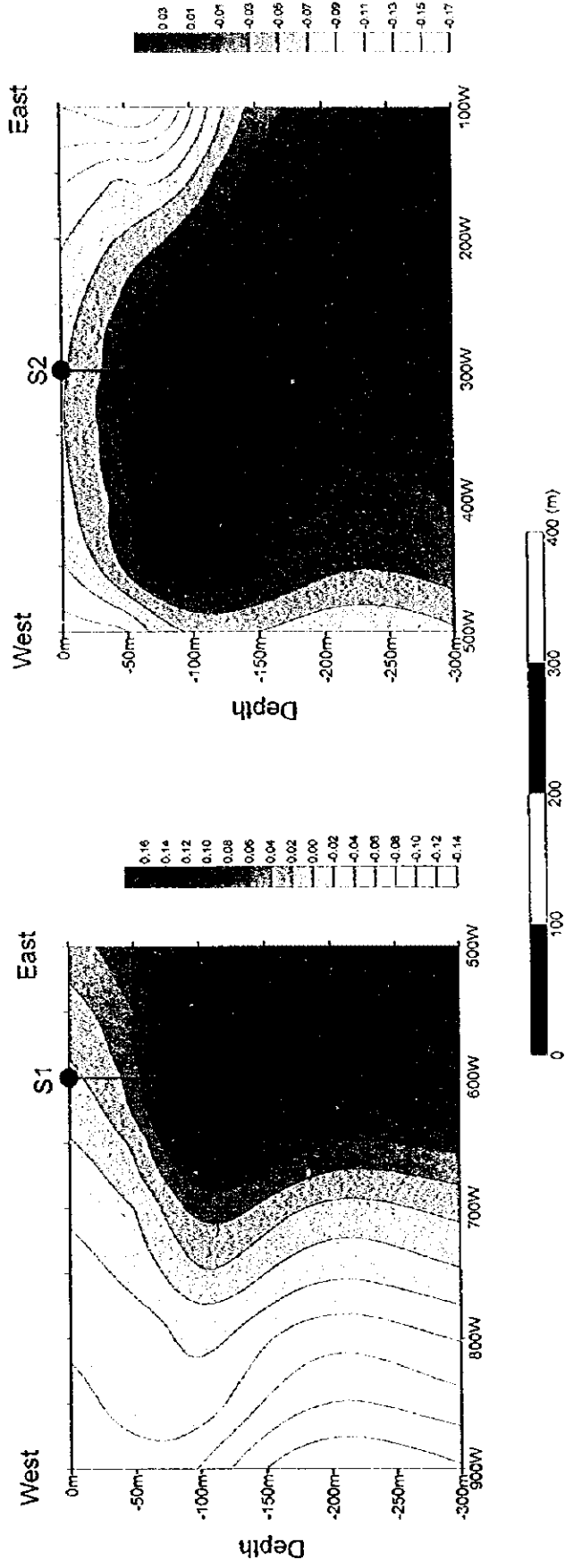


Fig. II -3-13 TEM response profile crossing drilling holes in Sarami area



during this field season.

Chargeability anomalies in Hara Kilab area were recognized in the west as well as in the central part. However, in the west part no massive sulphide can be expected because it corresponds to the V1-1 formation. The anomaly detected in the central part, where V1-2 is distributed, shows zones of relatively low resistivities with more or less high metal factor values. To clarify this anomaly, TEM survey was carried out on the locations indicated in Fig. II-2-23 and which cover an extension of about 800m by 800m.

(2) Results

Loop 1

Figures II-3-14(1) and II-3-14(2) show the contour maps of the TEM responses for each of the 20 channels. High TEM responses were detected in two zones: 1) between the coordinates 1350E2200N and 1500E1800N, and 2) upper right part of the loop. The anomaly detected in 1) is seen in the channels 1 to 8 and considered due to the influence of the underground waters, while the anomaly detected in 2) is seen clearly after channel 13, however this is not a distinctive anomaly that could lead to massive sulphide deposits.

Loop 2

Figures II-3-15(1) and II-3-15(2) show in plan view the contour maps of the TEM responses for each of the 20 channels. High TEM responses are seen increasing gradually to the right side of the loop and in particular the TEM response seems to increase monotonously from channel 11. A conductive body seems to exist to the right of this loop, however this anomaly is not indicative of any massive sulphide deposit inside of this loop.

Loop 3

Figures II-3-16(1) and II-3-16(2) show in plan view the contour maps of the TEM responses for each of the 20 channels. In the direction from the upper left to the lower right, a high TEM response seems to extend from channels 9 to 17. This anomaly corresponds to the high metal factor detected from the TDIP survey and related to mineralization.

To confirm this anomaly, the borehole MOJB-H2 was drilled, but it intersected only pyrite disseminations and veinlets with intense silicification and argillization, as described in more detail in Chapter 4 (Section 4-4-3).

Loop 4

Figures II-3-17(1) and II-3-17(2) show the contour maps of the TEM responses for each of the 20 channels. In the left side of this loop an anomaly of high TEM responses is seen along an up-low direction from the channels 9 to 16. As same as the anomaly detected in loop 3, it corresponds to the high metal factor values detected in the TDIP survey and suggests to be related to mineralization.



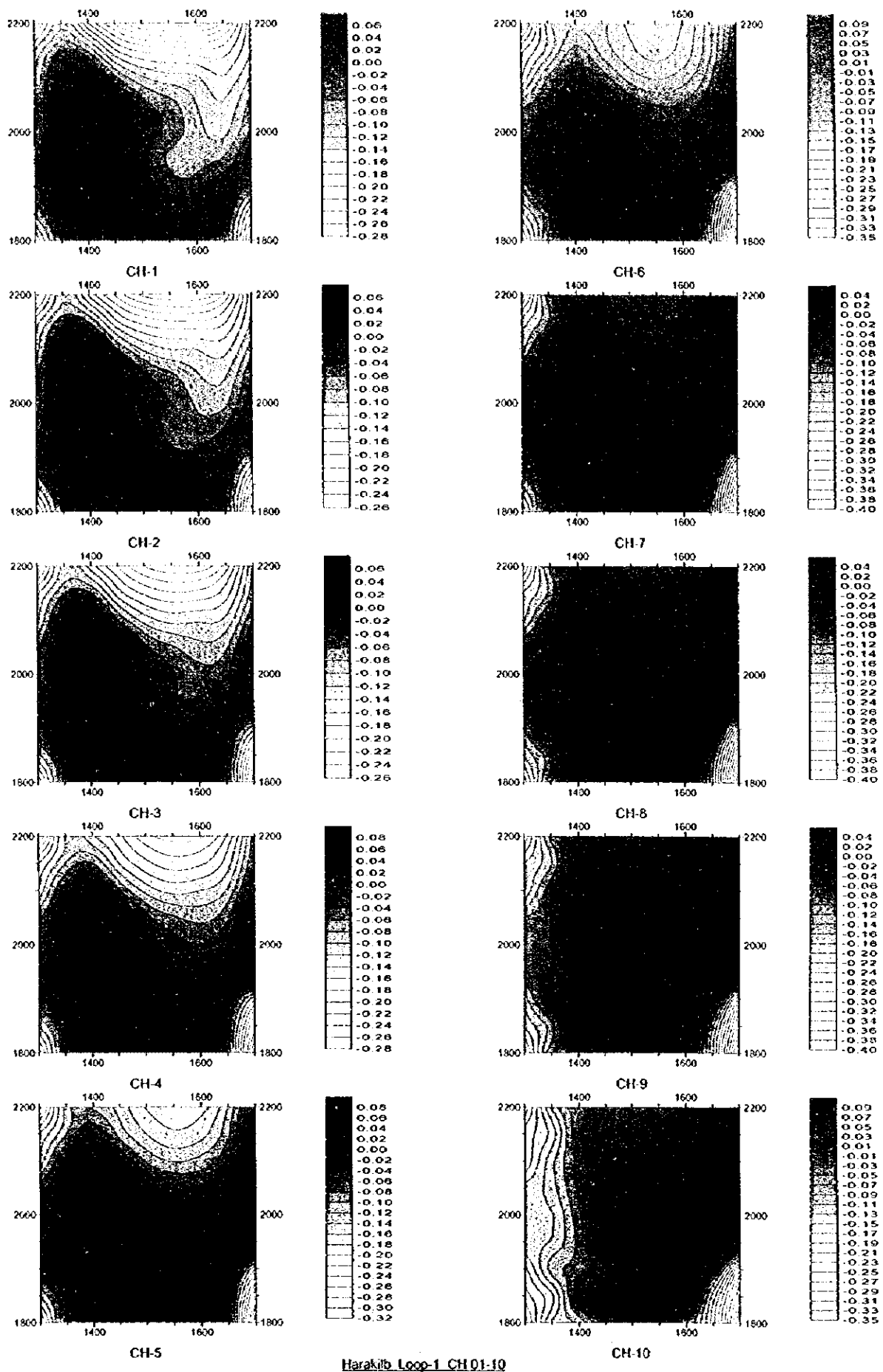


Fig. II -3-14(I) TEM response maps of Loop I in Hara Kilab area(CH1-CH10)



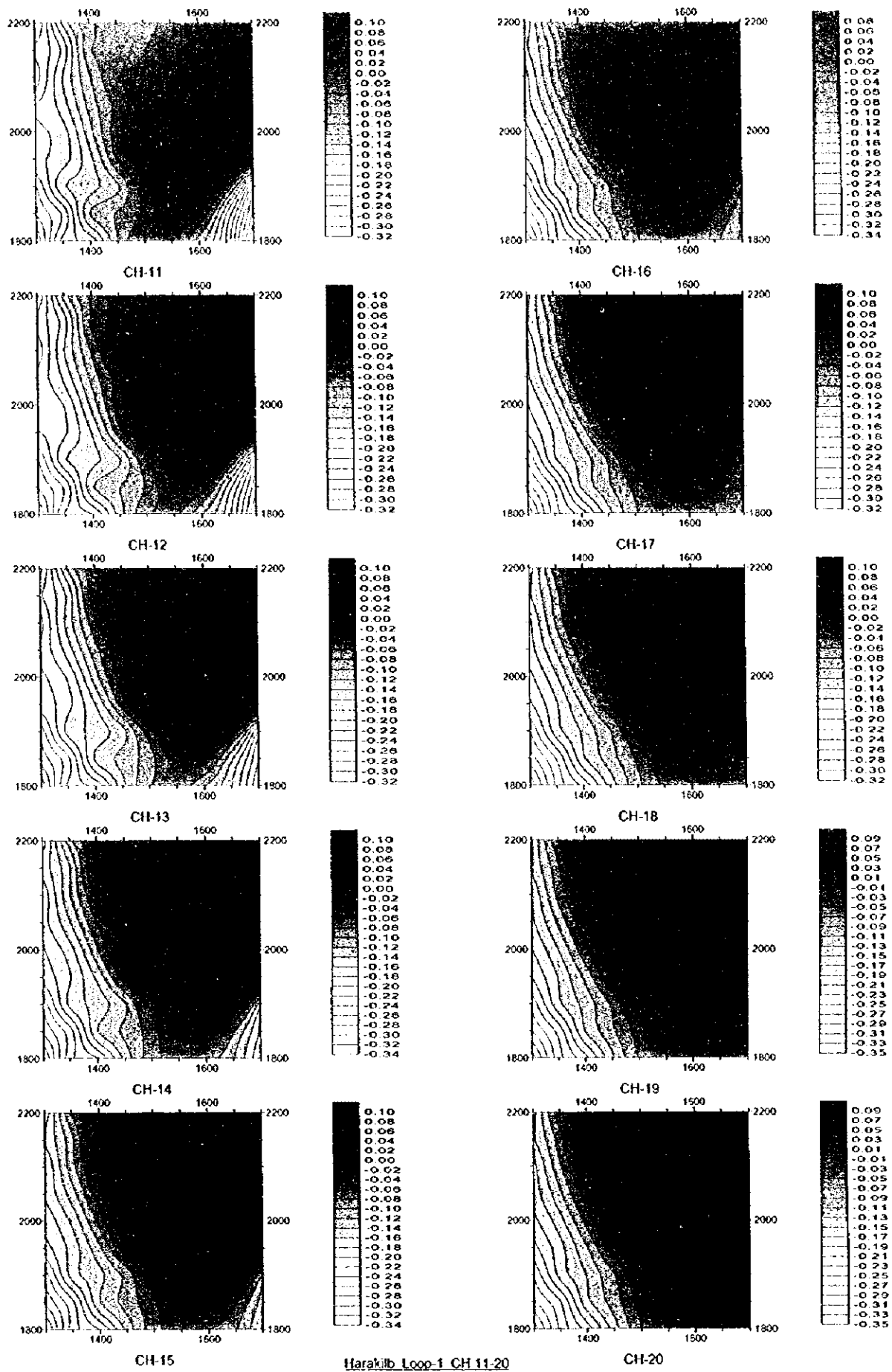
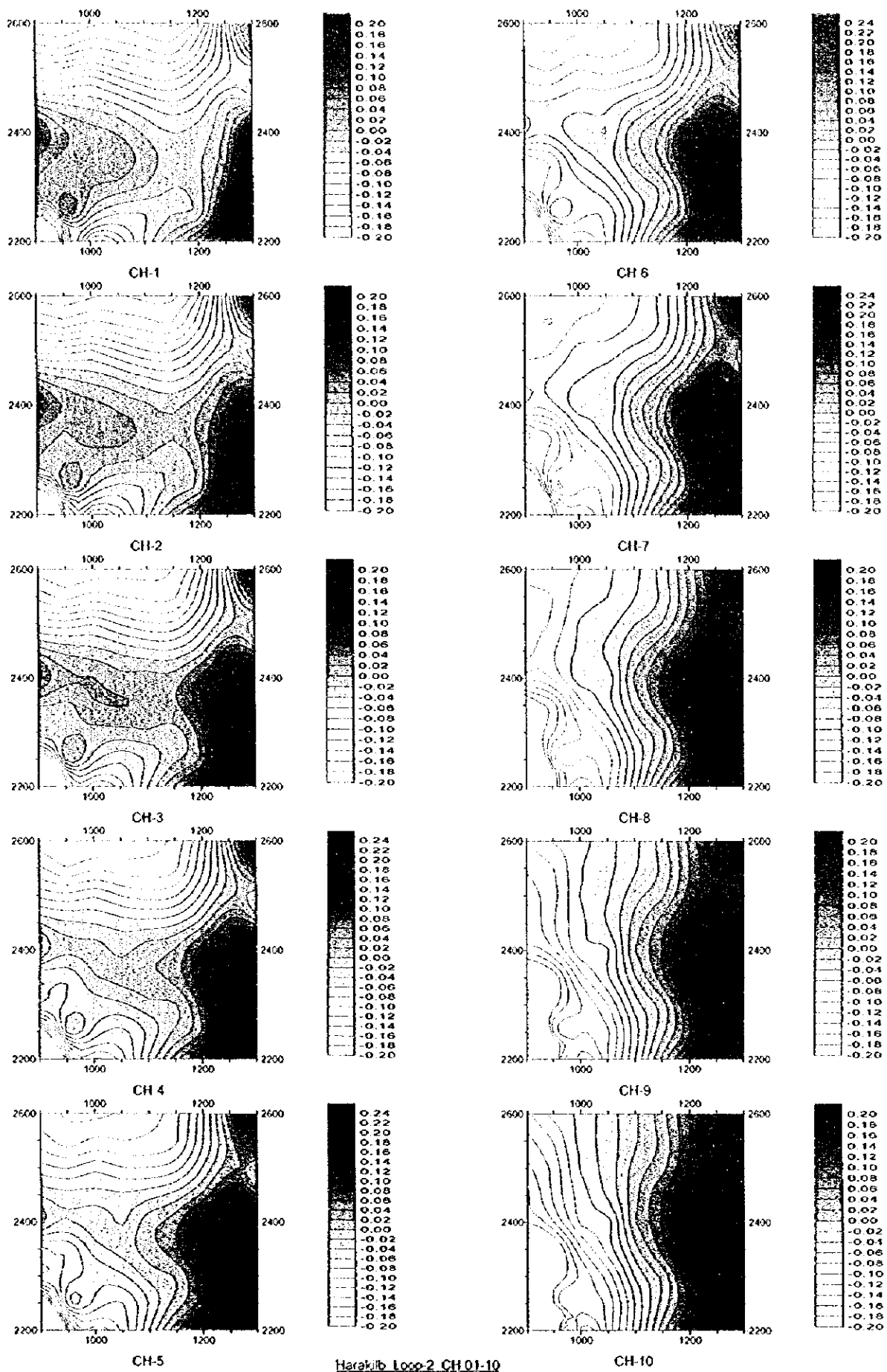


Fig. II-3-14(2) TEM response maps of Loop1 in Hara Kilab area(Ch11-Ch20)





Harakilb Loop-2 CH-01-10

Fig. II -3-15(1) TEM response maps of Loop2 in Hara Kilab area(Ch1-Ch10)



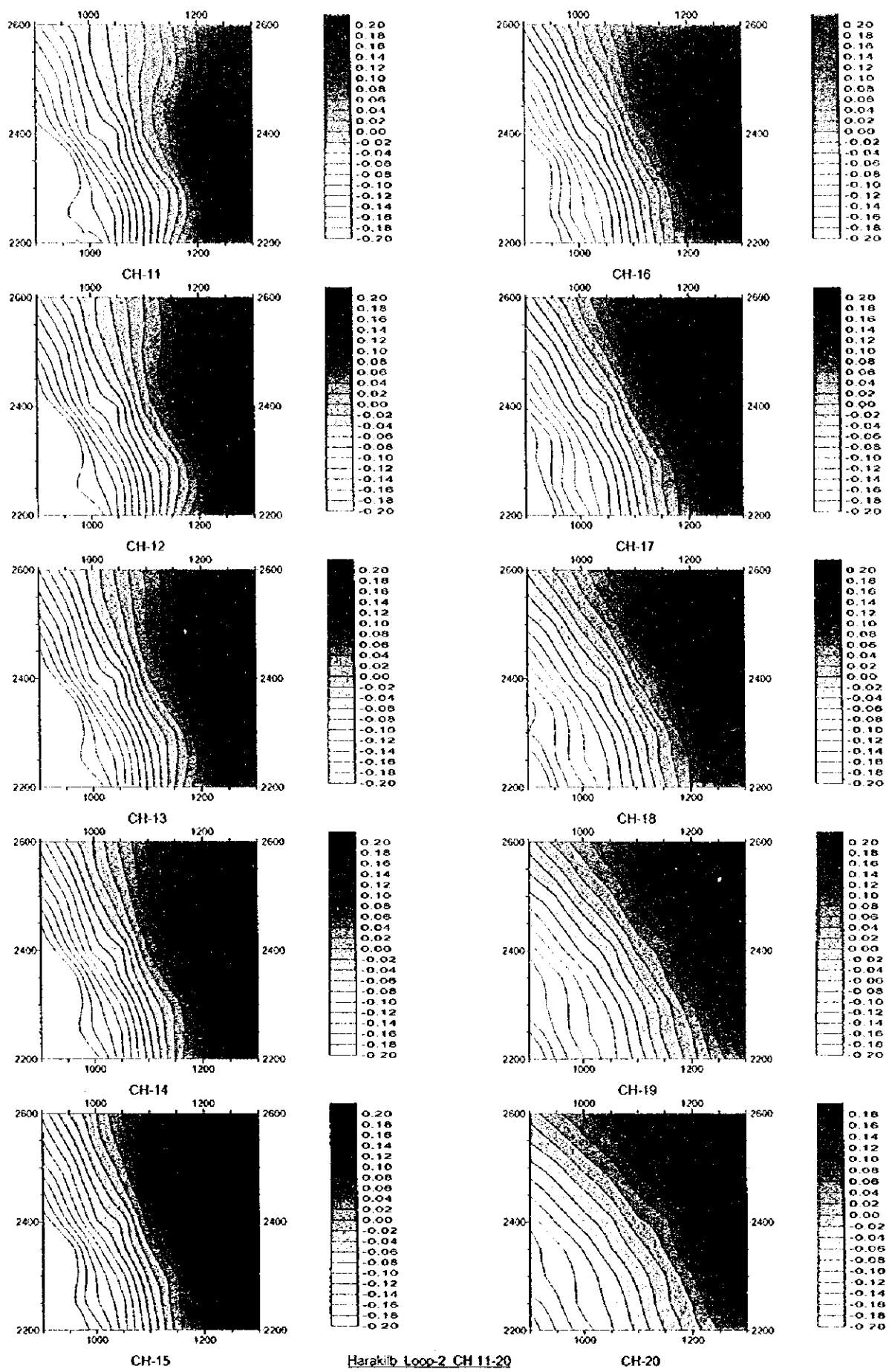


Fig. II-3-15(2) TEM response maps of Loop2 in Hara Kilab area(Ch11-Ch20)



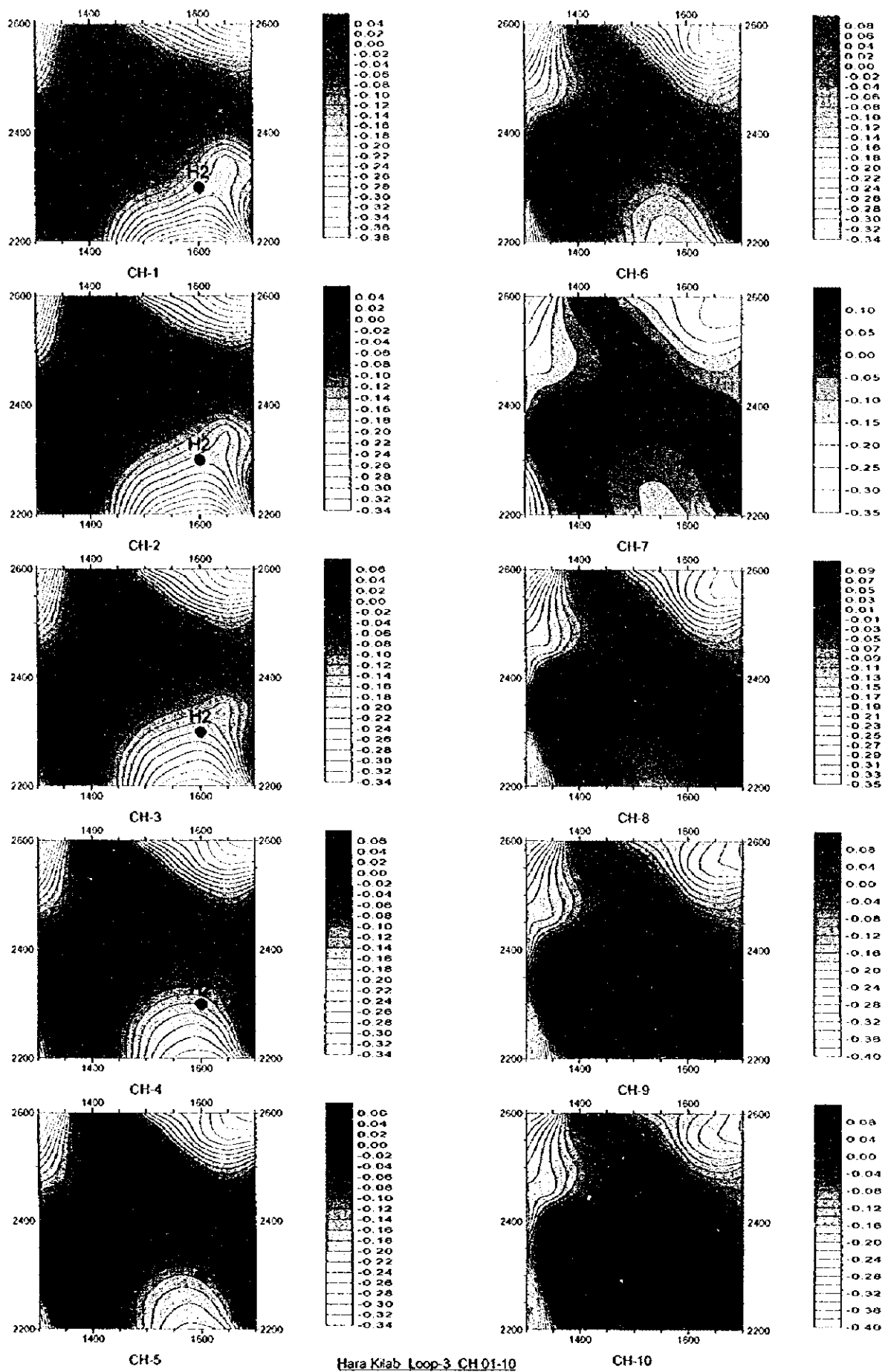


Fig. II-3-16(I) TEM response maps of Loop3 in Hara Kilab area(Ch1-Ch10)

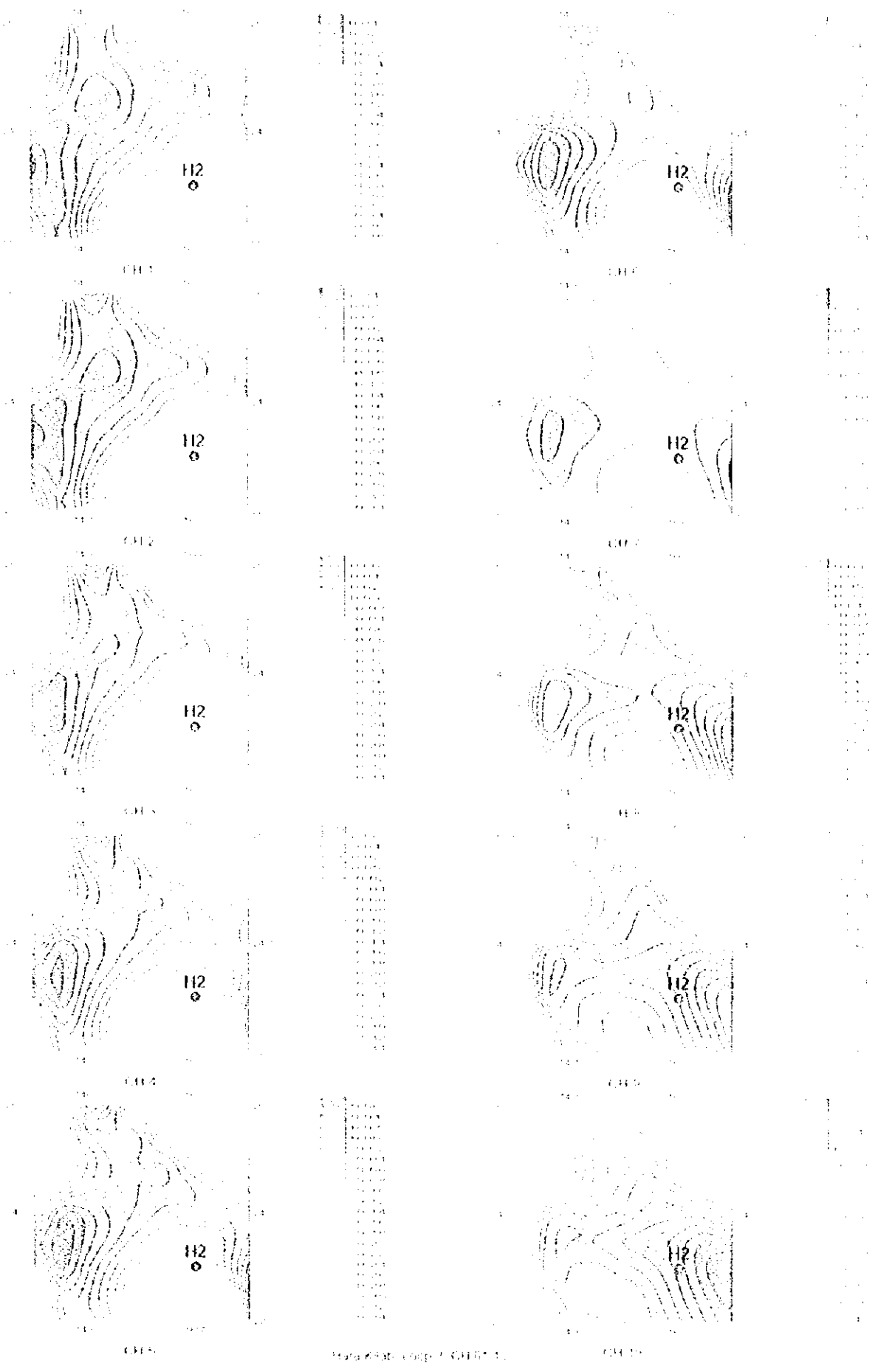


Fig. II-5-16(1) H₂M response maps of Loop 5 in Hara-Kilab area (CH1-CH10)



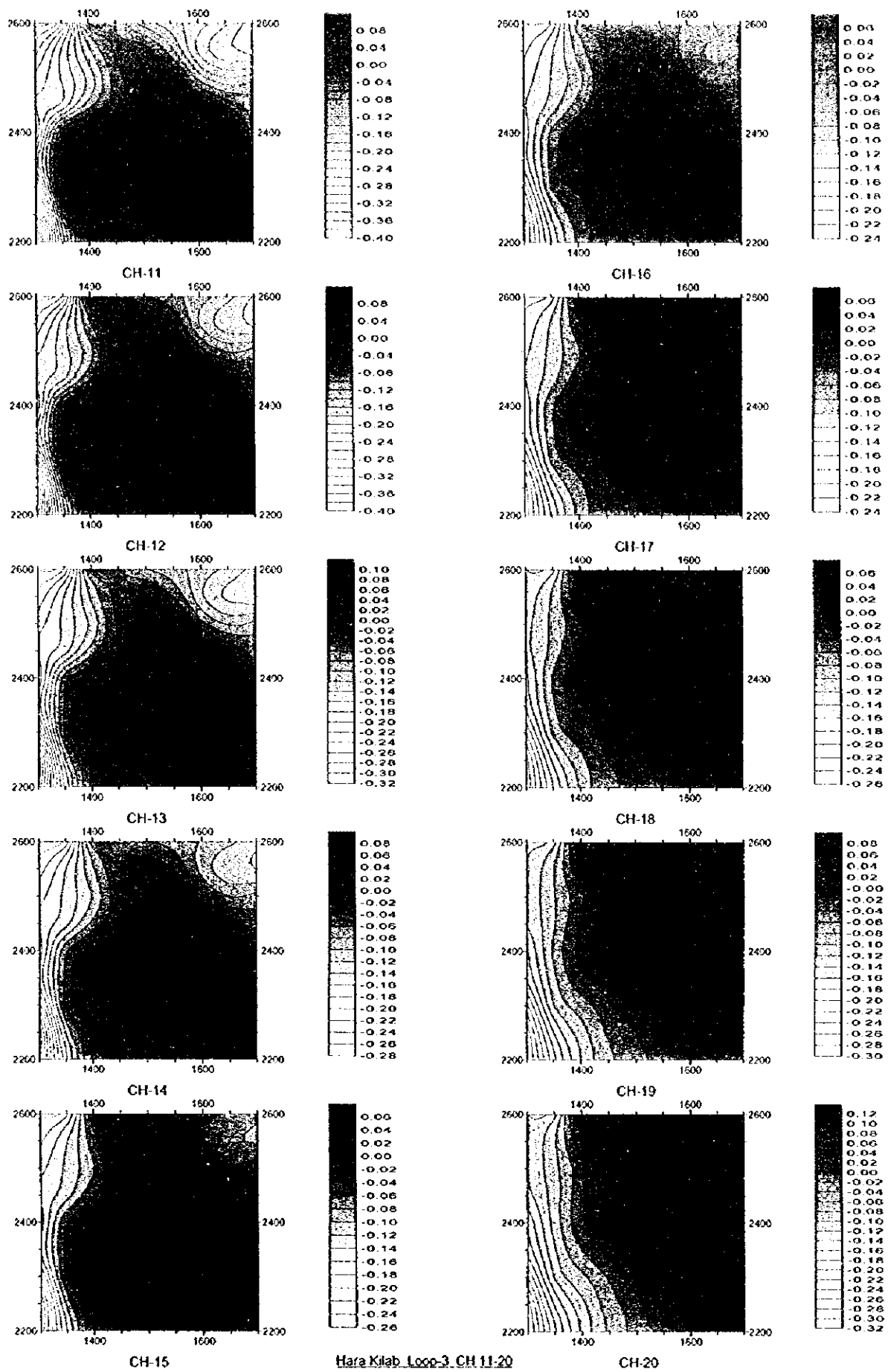


Fig. II -3-16(2) TEM response maps of Loop3 in Hara Kilab area(Ch11-Ch20)

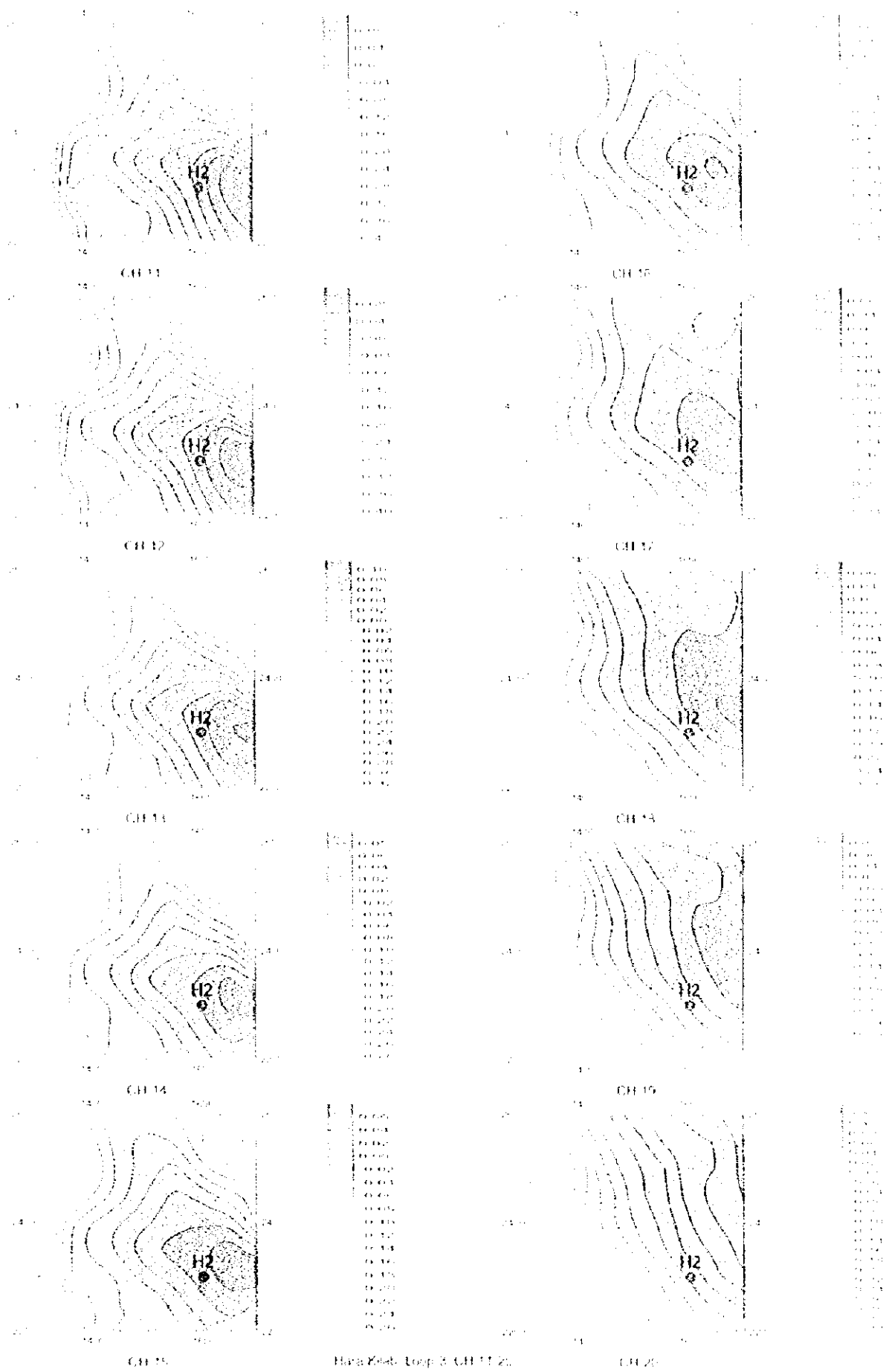
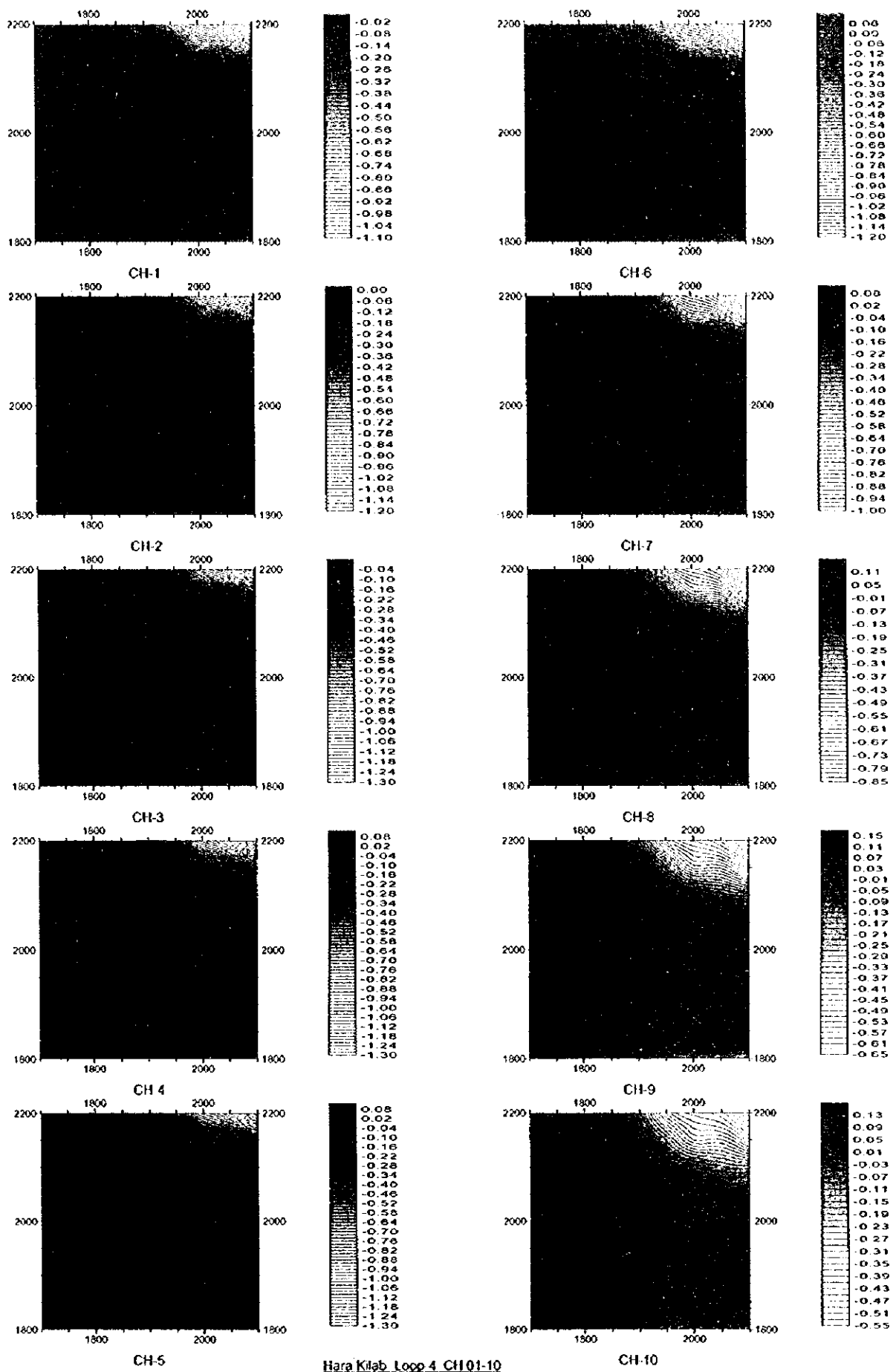


Fig. II-3-(6c) EMI response maps of Loop 3 in Data Kilaly area (Left-Ch20)





Hara Kilab Loop 4 CH01-10

Fig. II-3-17(I) TEM response maps of Loop4 in Hara Kilab area(CH1-Ch10)

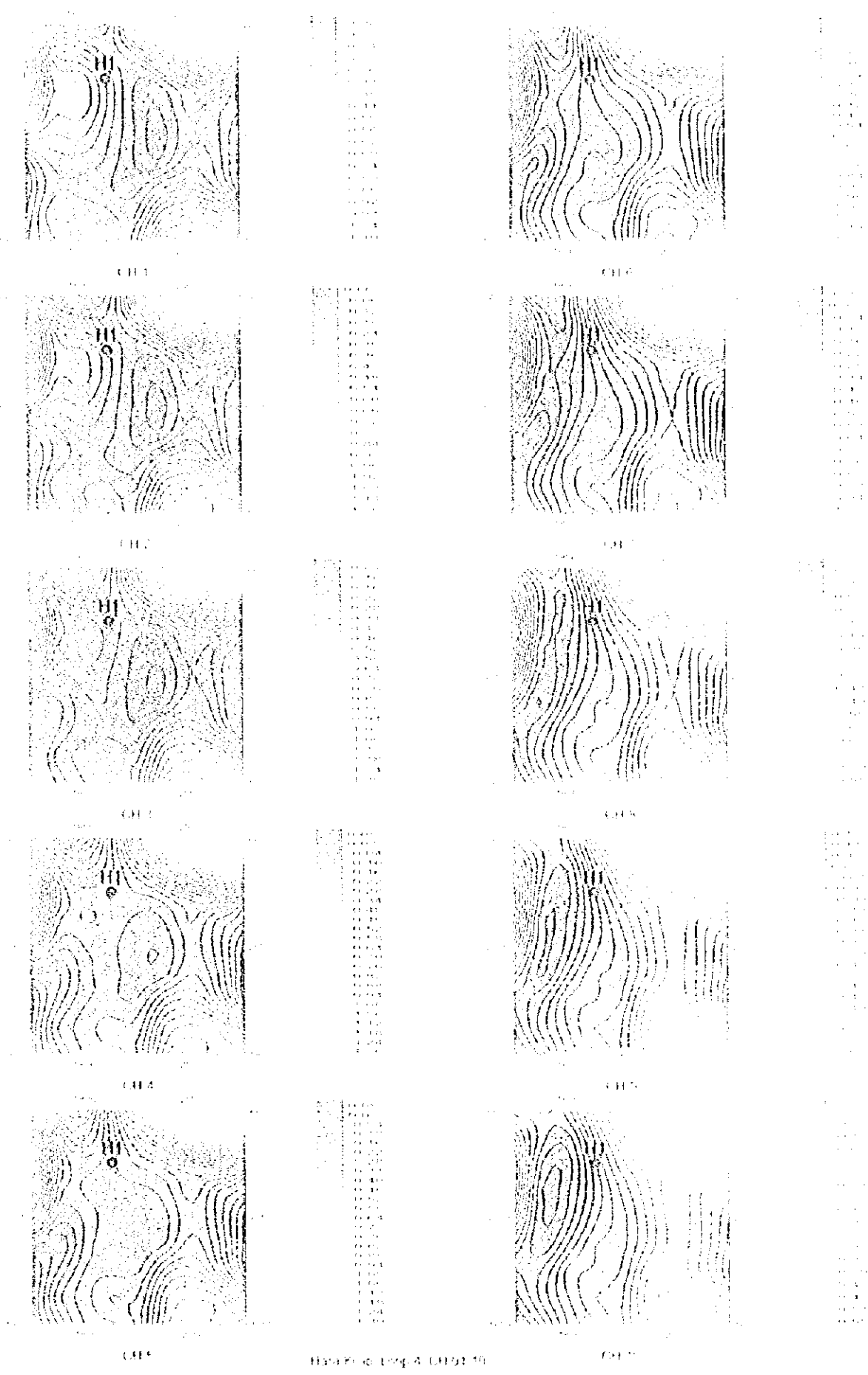
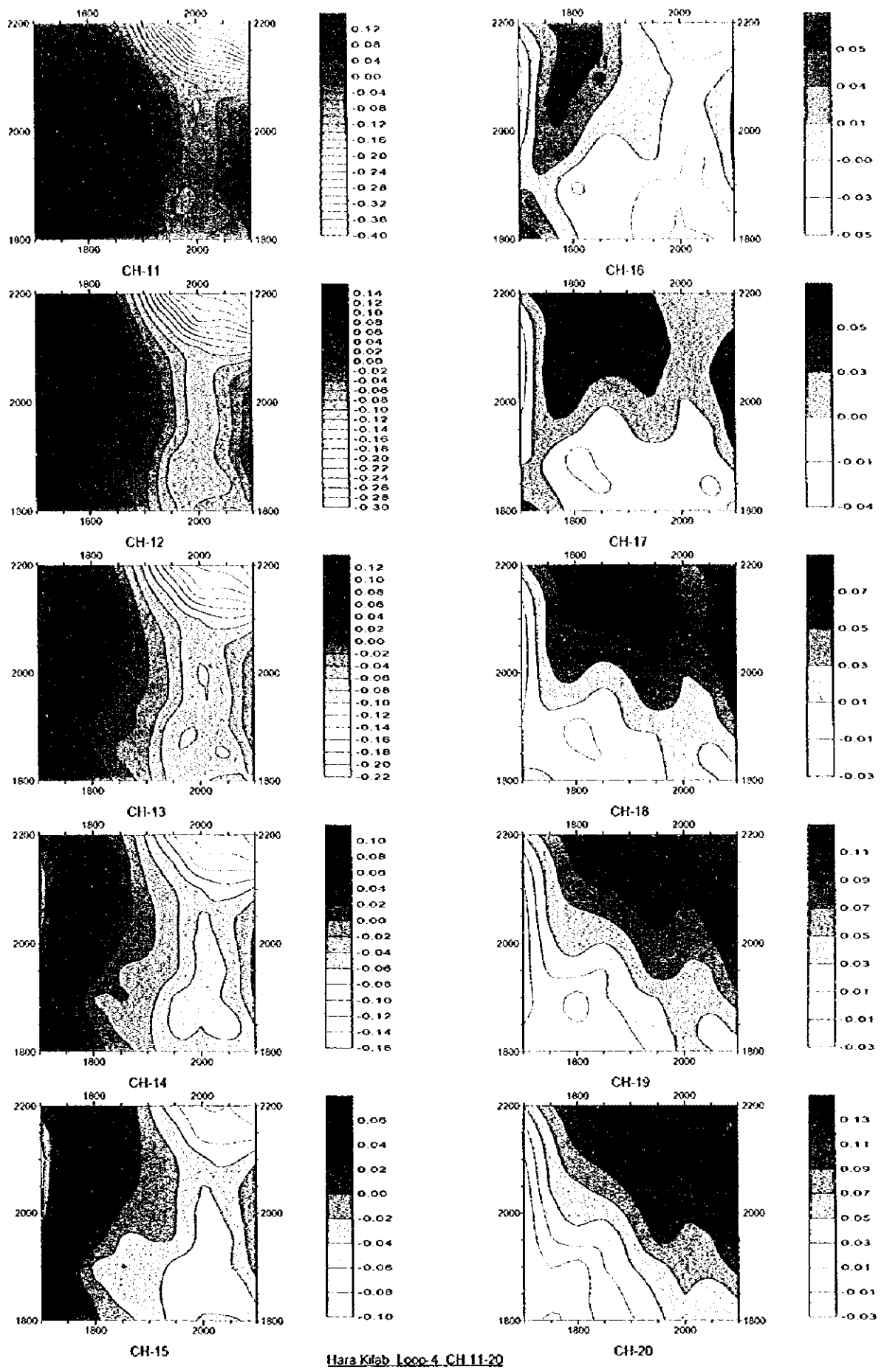


Fig. B-3. EM response maps of Loop 1 in Bara Khab area (CH1-CH10).





Hara Kilab Loop 4 CH 11-20

Fig. II-3-17(2) TEM response maps of Loop4 in Hara Kilab area(Ch11-Ch20)

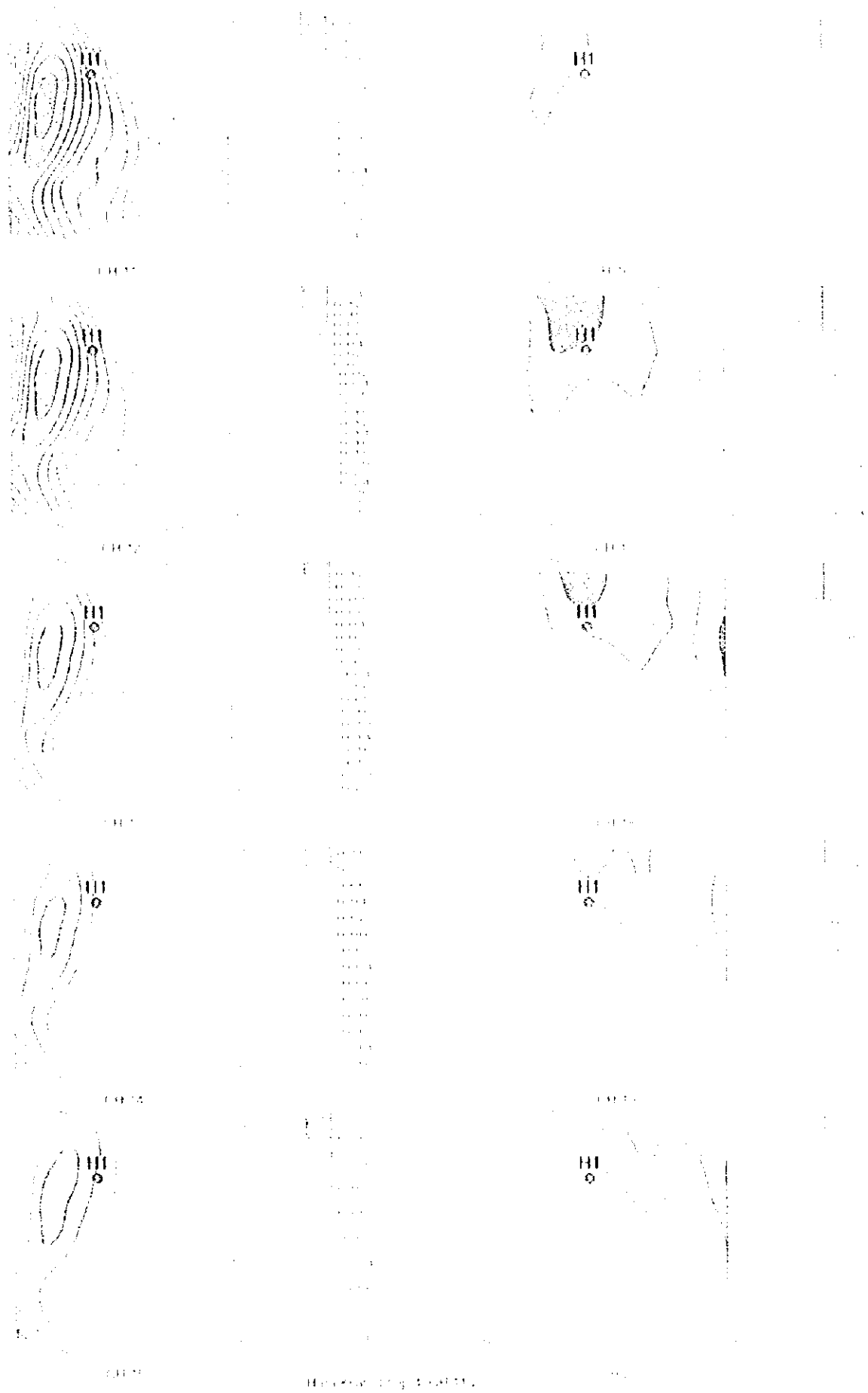


Fig. 11-8-37(2) IEM response maps of Loop1 in Hina-Kidab area (H1-C120)



To confirm this anomaly, the borehole MJOB-III was drilled, but it intersected only pyrite disseminations and veinlets with intense silicification and argillization, as described in more detail in Chapter 4 (Section 4-4-3).

Loop 5

Figures II-3-18(1) and II-3-18(2) show the contour maps of the TEM responses for each of the 20 channels. In general, low TEM responses are seen in this loop. Relatively high TEM responses are seen, however, in the lower left from the channels 3 to 13. Especially, in the central around the point 2000E2400N low TEM responses are detected and corresponding to high resistivity distribution. No indications of the existence of any massive sulphide deposit are seen in this loop.

Fig. II-3-19 shows 2 profiles of the TEM responses obtained around the boreholes MJOB-H1 and MJOB-H2.

3-6 Further Considerations

Regarding Mahab and Maqail areas refer to further considerations in Chapter 2 (Section 2-6).

3-6-1 Ghuzayn area

Fig. II-3-20 shows the compiled geophysical map obtained in Ghuzayn area. The upper figure in Fig. II-3-20 indicates the TDIP results, while the lower figure shows the TEM results. Both of them present the geophysical information to a depth of about 150 to 200m.

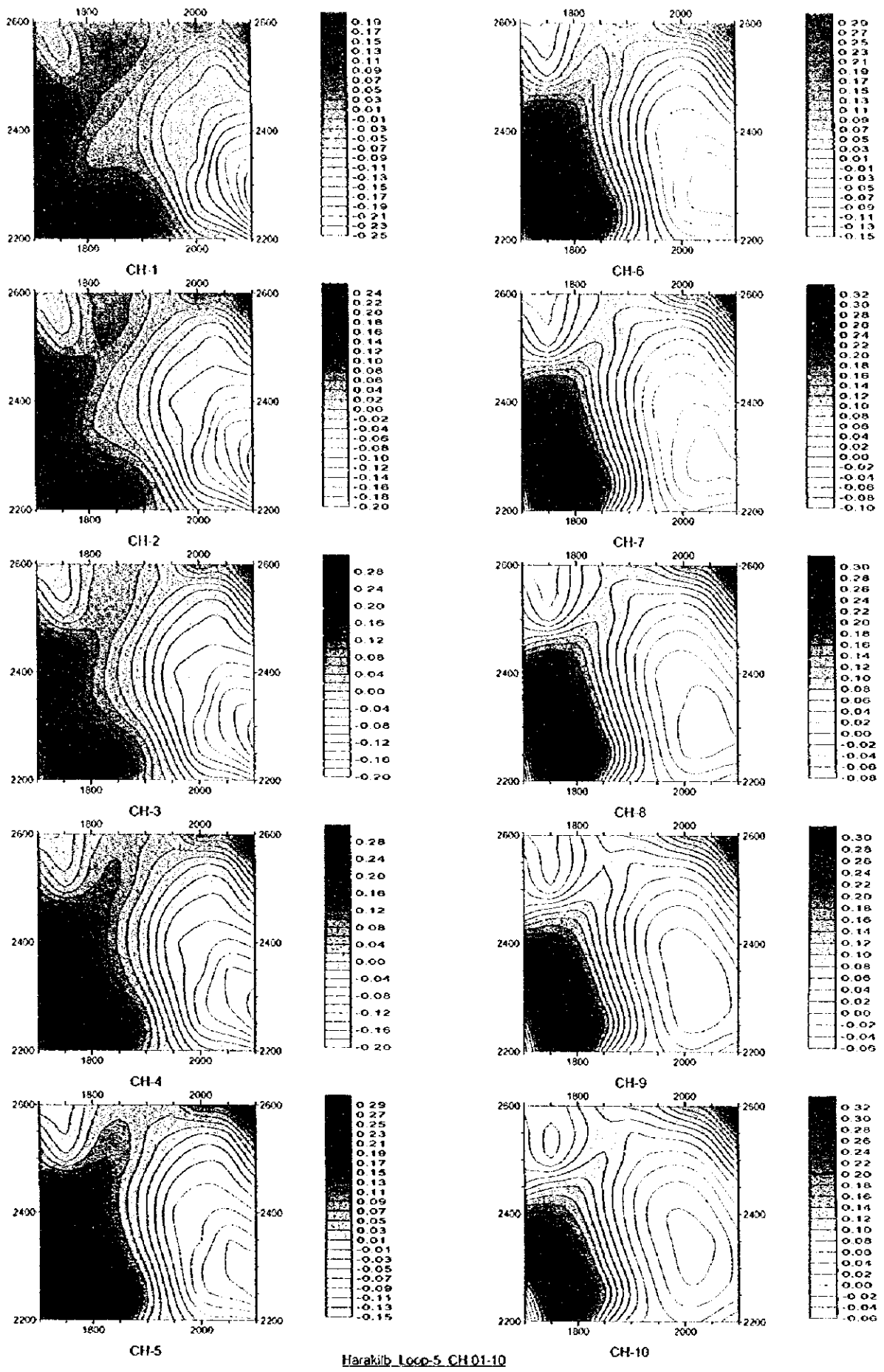
The IP results of Fig. II-3-20 indicate high chargeability zones of more than 8 mV/V detected in five locations: one in the western, three in central and one more in the eastern. Among them, high metal factor zones of more than 25 are seen in the west and central part. It is worthy to mention here that the high metal factor is a very important parameter to be considered here because the recently discovered ore bodies No.1 to No.3 are located not only in high chargeability zone but also within low resistivity zone.

The high chargeability zone widely detected in the western part in the area indicates the possible existence of deposits. There is a possibility for the existence of stockwork type deposits in this zone, but unlikely to find massive sulphide deposits because the zone where the high metal factor is extended is narrow in comparison with that in the central part where the massive sulphide ore bodies No. 1 to No.3 were discovered.

The compiled TEM results carried out in selected zones are presented in Fig. II-3-18. In this figure, the dark green parts represent high TEM responses, which coincide in general with the zones where the massive sulphide deposits were discovered.

The results of the TEM survey conducted in the western part of the area did not show any significant TEM response that could confirm the existence of massive sulphide deposits. However, as described above there is possibility of existence of stockwork type deposits, taking into account that the high chargeability zone is widely distributed outside of the TEM surveyed location.





Harakilb Loop-5 CH01-10

Fig. II-3-18(1) TEM response maps of Loop5 in Hara Kilab area(Ch1-Ch10)



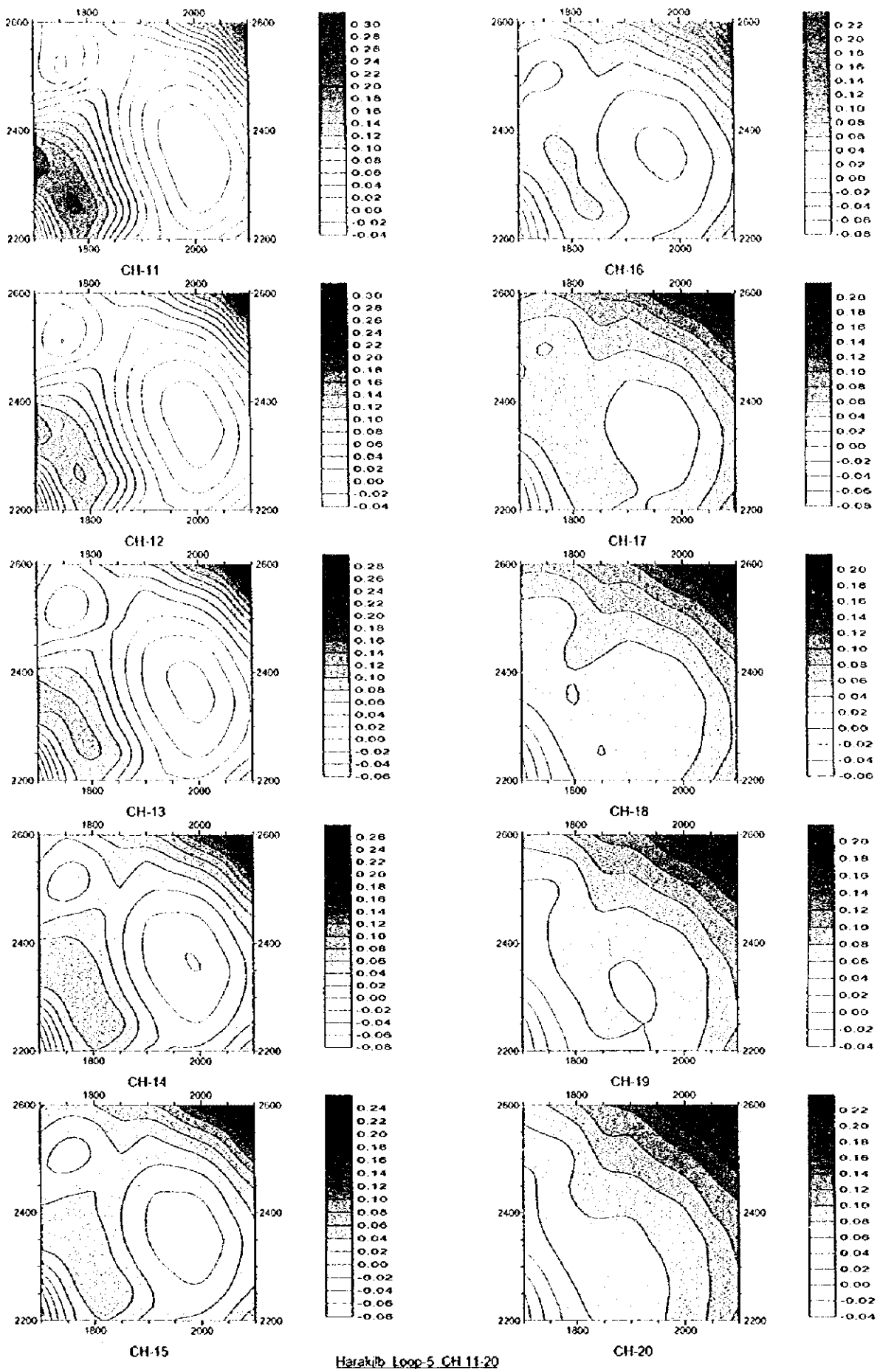


Fig. II -3-18(2) TEM response maps of Loop5 in Hara Kilab area(Ch11-Ch20)



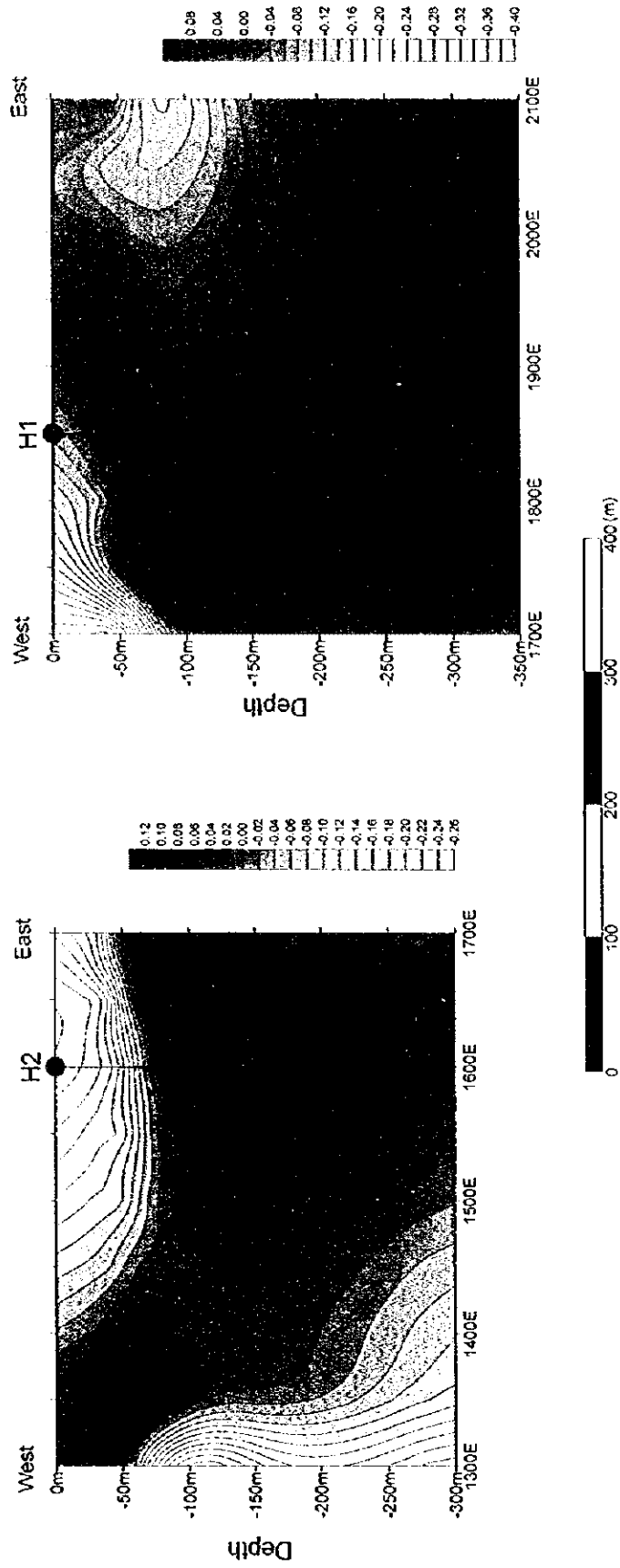


Fig. II-3-19 TEM response profile crossing drilling holes in Hara Kilab area



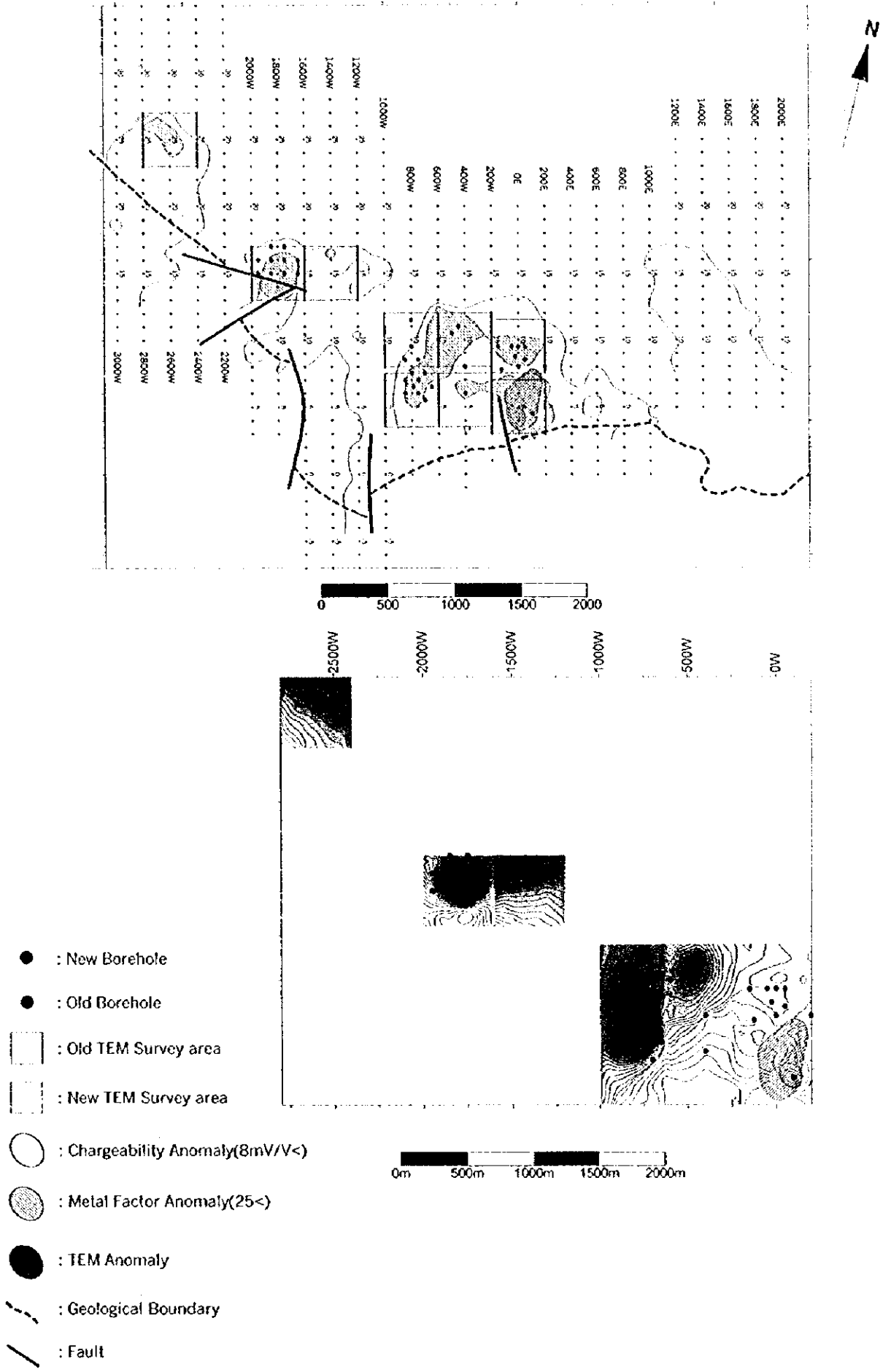


Fig. II-3-20 Compiled geophysical map in Ghuzayn area

